

## BACHELOR

### Diffusion of a Passive Tracer in an Active Crowded Environment

van Dijk, F.

*Award date:*  
2020

[Link to publication](#)

#### **Disclaimer**

This document contains a student thesis (bachelor's or master's), as authored by a student at Eindhoven University of Technology. Student theses are made available in the TU/e repository upon obtaining the required degree. The grade received is not published on the document as presented in the repository. The required complexity or quality of research of student theses may vary by program, and the required minimum study period may vary in duration.

#### **General rights**

Copyright and moral rights for the publications made accessible in the public portal are retained by the authors and/or other copyright owners and it is a condition of accessing publications that users recognise and abide by the legal requirements associated with these rights.

- Users may download and print one copy of any publication from the public portal for the purpose of private study or research.
- You may not further distribute the material or use it for any profit-making activity or commercial gain

# Diffusion of a Passive Tracer in an Active Crowded Environment

Bachelor Final Project

Friso van Dijk (1265989)

*Supervisors:*

Dr. Oliver Tse,

Dr. Liesbeth Janssen,

Prof. Dr. Ir. Paul van der Schoot,

Dr. Alexey Lyulin



Eindhoven University of Technology  
Departments of Mathematics and Computer Science  
Department of Applied Physics  
July 2020

## Abstract

Active Brownian particles are Brownian particles that can take up energy from their environment and use it to propel themselves. This is contrary to passive Brownian particles, which can only diffuse through thermal fluctuations in the fluid in which they are suspended. Hence, active Brownian particles move through a fluid by two mechanisms: by diffusion and by self-propulsion. Bacteria and algae form examples of active Brownian particles. In this report, we investigate the dynamics of a single passive Brownian particle (a *tracer*) in a crowded environment of active particles. All particles interact via a short-range, repulsive potential, and hydrodynamic interactions are neglected. We investigate the tracer's mean-squared displacement (MSD) as a function of time and study how activity, temperature and density influence the tracer's dynamics. This is done in two ways: first, we use the mathematical formalism of stochastic differential equations and Itô calculus, and a series of approximations to find an analytical expression for the MSD. Secondly, we simulate the system numerically using Brownian dynamics simulations and calculate the MSD from the results of these simulations. In both methods, we find that the active bath dramatically enhances the tracer's diffusion. However, the analytical approximations predict long-time ballistic motion, whereas the numerical simulations show that the tracer diffuses linearly at these time scales. Furthermore, the simulations show superdiffusive or subdiffusive behaviour at intermediate time scales, where  $\text{MSD}(t) \sim t^\alpha$  with  $\alpha > 1$  or  $\alpha < 1$  respectively, depending on activity. This behaviour is not predicted by the analytical methods. We expect that these discrepancies are due to the approximations made in the analytical MSD calculation.

# Contents

<b>1</b>	<b>Introduction</b>	<b>2</b>
1.1	Structure of the report . . . . .	4
1.2	Notation . . . . .	4
<b>2</b>	<b>Stochastic Differential Equations</b>	<b>5</b>
2.1	Brownian motion . . . . .	5
2.2	Stochastic differential equations . . . . .	6
2.3	The Itô integral . . . . .	7
2.4	Diffusion processes . . . . .	10
2.5	An important example . . . . .	10
2.6	Active matter . . . . .	11
<b>3</b>	<b>Model description</b>	<b>16</b>
3.1	Model . . . . .	16
3.2	Brownian dynamics simulations . . . . .	18
<b>4</b>	<b>Analytical Approximation of the MSD</b>	<b>21</b>
4.1	Probability density of the tracer . . . . .	21
4.2	Probability density of a host particle . . . . .	26
4.3	MSD estimation . . . . .	28
4.4	Approximation of host particle density function by matched asymptotic expansions . . . . .	32
<b>5</b>	<b>Simulation Results</b>	<b>36</b>
5.1	Short-time regime . . . . .	36
5.2	Intermediate regime . . . . .	37
5.3	Long-time regime . . . . .	39
<b>6</b>	<b>Conclusion and Outlook</b>	<b>42</b>
6.1	Comparison of the analytical and simulation results . . . . .	42
6.2	Outlook . . . . .	43

# Chapter 1

## Introduction

Active Brownian particles are particles that are suspended in a fluid and that can take up energy from their environment and use it to drive themselves [1]. This property distinguishes active Brownian particles from passive Brownian particles, which only move through the fluid because of the thermal fluctuations in the fluid. Due to their activity, these particles are never in equilibrium with their environment [1]. Moreover, because of their self-propulsion, active Brownian particles diffuse much faster than their passive counterparts. On the other hand, a *passive* Brownian particle in an environment that is crowded by other passive Brownian particles, diffuses much more *slowly* than if it could diffuse freely [2–4].

The collective motion of active Brownian particles can give rise to fascinating phenomena. For instance, the dynamics of schools of fish and flocks of birds are modelled using the theory of active matter [5, 6]. Active matter is also observed on the microscopic scale. Bacteria can propel themselves, for instance using flagella, as a more efficient means for finding food. On the other hand, artificial, non-living microscopic particles can also show active motion. For example, gold-platinum microrods can induce concentration gradients in hydrogen peroxide solutions, thereby significantly enhancing their directed motion [1]. Because of these remarkable properties, active matter has become an active research topic in the (bio)physics community [7].

In this report, we investigate the influence of active Brownian particles on passive ones. In particular, we will consider a two-dimensional bath of active particles (‘hosts’) in which a single passive particle (‘tracer’) is submerged. All particles interact via a short-range, repulsive potential. The first experiment on this type of system, with a small number passive particles surrounded by active particles, was conducted in 2000 by Wu and Libchaber [8]. They found that the tracer to some extent inherits the activity of the hosts, which dramatically changes diffusive behaviour. For instance, for long times, the tracer diffuses as it would in a bath with a temperature about a hundred times larger than the actual bath temperature. Soon after, numerical simulations could reproduce these results [9]. Numerous other physical and numerical experiments have been performed since for similar systems, all indicating the same enhanced diffusion of the tracer, see e.g. [10–12].

At low densities, hydrodynamic interactions between the hosts and the tracer are thought to be responsible for the tracer’s enhanced diffusivity [13]. This

means that when an (active) Brownian particle attains a velocity, it induces a flow field in the liquid, that affects the motion of the other Brownian particles [14]. However, in this report we neglect these interactions, and only consider the repulsive, direct interactions between tracer and host and between hosts themselves. Moreover, in highly crowded environments the hydrodynamic interactions can cancel if now global flow is built up [1].

The goal of this report is to investigate the mean squared displacement ( $\text{MSD}(t) := \mathbb{E}[|\mathbf{X}_t - \mathbf{X}_0|^2] := \langle |\mathbf{X}_t - \mathbf{X}_0|^2 \rangle$ , where  $\mathbf{X}_t$  is the position of the particle at time  $t$  and  $\mathbf{X}_0$  is its initial position) of a passive Brownian tracer in an active bath. The MSD is the conventional quantity to probe the dynamics of a Brownian particle. More specifically, we want to know how the MSD depends on the bath activity, temperature and host particle concentration. We find that at very short times  $\text{MSD}(t) \sim t$  (in the overdamped limit), at intermediate times  $\text{MSD}(t) \sim t^\alpha$ , with  $\alpha < 1$  or  $\alpha > 1$  depending on the ratio  $v_0/T$ , and at long times  $\text{MSD}(t) = D_{\text{eff}}t$ , where  $D_{\text{eff}}$  is an effective diffusion coefficient. We investigate how the values of  $\alpha$  and  $D_{\text{eff}}$  depend on the aforementioned quantities.

We approach the problem in two different ways: analytically and numerically. For the analytical route, we first need to understand the theory of stochastic differential equations (SDEs) and Itô calculus. The solutions of ordinary (or partial) differential equations are fully deterministic; for example, given initial conditions, Newton's laws predict precisely the motion of an object in a gravitational field, and each time we perform the same experiment and we measure the trajectory of the object, we find exactly the same results. However, the solutions of stochastic differential equations are random variables. For example, the motion of a particle in a fluid is modelled using SDEs, since the particle will follow a different, random trajectory each time we let it diffuse in the fluid. The particles that we consider follow random trajectories because of their collisions with the molecules of the fluid in which they are suspended. With this new type of differential equations comes a new type of integration: we will define the Itô integral to be able to solve SDEs.

Moreover, to each SDE we can, under some conditions, associate a partial differential equation for the probability density of the solution of the SDE. These partial differential equations are called Fokker-Planck equations; they describe the evolution of the probability density in space and time. Hence, the random motion of particles can be described in two different formulations: on the microscopic level, we describe the random motion of all particles using SDEs; on the macroscopic level, we describe the probability density of these particles using the Fokker-Planck equation associated with the SDEs.

For the numerical simulations, we use the SDE level: using Brownian dynamics simulations, we simulate the random motion of each of the particles in the system and calculate the tracer's MSD from the results of these simulations. On the other hand, we use the macroscopic, Fokker-Planck description to find an analytical approximation for the probability density of the tracer. Multiplying this density by the square of the tracer's position and integrating over all space yields the (approximate) MSD.

## 1.1 Structure of the report

Chapter 2 focuses on Itô calculus and stochastic differential equations. The first SDE we study is the one that describes the random motion of a particle suspended in a fluid. Next, we describe SDEs that model more general motion, for instance that of interacting active particles. Furthermore, we discuss the Itô integral, which is necessary to find solutions SDEs, and provide a theorem that converts SDEs to Fokker-Planck equations. These SDEs will be used throughout the report to describe our models. In Chapter 3 we describe the model we use for numerically simulating the random evolution of particle system, and we outline the methods used for this. In Chapter 4 an approximate solution to the PDE that governs the tracer's probability density is presented and the tracer's MSD is calculated from this, whereas in Chapter 5 the results of the numerical simulations are given. We finish with a conclusion and outlook in Chapter 6, which also compares the results from the two approaches.

## 1.2 Notation

We mostly use the notation and terminology that is conventional in mathematics.

- The expectation value of a random variable  $X$  is written as  $\mathbb{E}[X]$ , rather than  $\langle X \rangle$ , which is more common in physics.
- For a random variable  $X$  that is distributed according some distribution  $\mathcal{A}$ , we write  $X \sim \mathcal{A}$ . In particular, if  $X$  follows a normal distribution with mean  $\mu$  and variance  $\sigma^2$ , we write  $X \sim \mathcal{N}(\mu, \sigma^2)$ .
- Vectors will be written in boldface. The inner product of two vectors  $\mathbf{x} = (x_1, \dots, x_n)$ ,  $\mathbf{y} = (y_1, \dots, y_n) \in \mathbb{R}^n$  is denoted by  $\mathbf{x} \cdot \mathbf{y} = x_1 y_1 + \dots x_n y_n$ .

## Chapter 2

# Stochastic Differential Equations

In this Chapter we introduce the reader to the mathematical preliminaries needed to understand the rest of this work. First, we define the Brownian motion (Definition 2.1), which is a continuous-time stochastic process that takes values in  $\mathbb{R}^n$ . Next we introduce the concept of stochastic differential equations (SDEs, Equation (2.8)), which can loosely be thought of as differential equations that contain a random noise term. Apart from physics, SDEs also find applications in stochastic finance. Subsequently we provide theorems and definitions necessary to solve SDEs, such as the Itô Integral (Definition 2.4), and Itô's formula (Theorem 2.7), which allows for a quick calculation of Itô integrals. The solution of an SDE is a stochastic process itself. In Theorem 2.10 we show how to convert an SDE into a PDE for the probability density functions of the solution of the SDE. In Section 2.5 we calculate the MSD of a freely diffusing passive particle, and in Section 2.6 we calculate the MSD of an active particle.

For this chapter we rely heavily on [15] and [16]. We refer to these books for proofs and more elaborate discussions.

### 2.1 Brownian motion

When a bead is suspended in a liquid and does not experience any external force, it performs a random, jittery movement. This movement is called *Brownian motion*, and we start by giving the axiomatic definition of the mathematical model for this.

**Definition 2.1.** Let  $(\Omega, \mathcal{F}, \mathbb{P})$  be a probability space. A *Brownian motion* or *Wiener process* is a continuous-time stochastic process  $\{B_t \mid t \geq 0\}$  such that

1.  $B_0 = 0$  almost surely,
2. The trajectory  $t \mapsto B_t$  is almost surely continuous,
3.  $B_t$  has independent increments, with  $B_t - B_s \sim \mathcal{N}(0, t - s)$  for  $t > s \geq 0$ .

Here  $X \sim \mathcal{N}(\mu, \sigma^2)$  means that the random variable  $X$  is normally distributed with mean  $\mu$  and variance  $\sigma^2$ .  $B_0 = 0$  almost surely means that the probability of  $B_0$  being nonzero is 0.



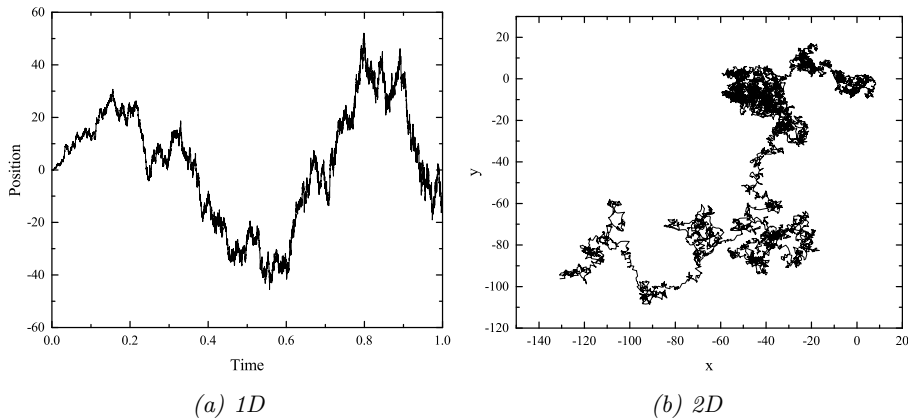


Figure 2.1: Sample paths of 1- and 2-dimensional Brownian motions. The paths are generated using the Karhunen-Loève expansion [16].

An  $n$ -dimensional Brownian motion is simply an  $n$ -dimensional vector of independent Brownian motions  $(B_t^1, \dots, B_t^n) \in \mathbb{R}^n$ . In Figure 2.1 example trajectories of 1 and 2-dimensional Brownian motions are given. The probability density function  $p : \mathbb{R}^n \times \mathbb{R}_+ \rightarrow \mathbb{R}$  of an  $n$ -dimensional Brownian motion is given by

$$p(\mathbf{x}, t) = \frac{1}{\sqrt{2\pi t}^n} \exp\left(-\frac{|\mathbf{x}|^2}{2t}\right), \quad (2.1)$$

for  $\mathbf{x} \in \mathbb{R}^n$  and  $t \in \mathbb{R}_+$ .

## 2.2 Stochastic differential equations

In physics literature, the equation of motion of a particle suspended in a liquid is usually described by a *Langevin equation* [14, 17], such as

$$m \frac{d^2 \mathbf{X}}{dt^2} = -\gamma \frac{d\mathbf{X}}{dt} - \nabla V + \sqrt{2\gamma k_B T} \eta(t). \quad (2.2)$$

This equation follows from Newton's second law. Here  $\mathbf{X}$  is the position of the particle. The term  $-\gamma d\mathbf{X}/dt$  represents the drag force on the particle and  $-\nabla V$  is the (external) conservative force.  $k_B$  is Boltzmann's constant, and  $T$  denotes the temperature. The term that we will be concerned with in this section is  $\eta(t)$ , which is a 'rapidly fluctuating force'. This force is the result of the continuous bombardment of the particle by the small molecules of the liquid. We do not know how  $\eta$  depends on time; we can only describe its statistical properties.  $\eta$  is delta-correlated. For instance, in two dimensions,  $\eta(s) = (\eta_1(s), \eta_2(s))$  and for  $i, j = 1, 2$

$$\mathbb{E}[\eta_i(t)\eta_j(s)] = \delta_{ij}\delta(t-s), \quad (2.3)$$

where  $\delta_{ij}$  is the Kronecker delta and  $\delta(s)$  is the Dirac delta function.

Now we assume that the ratio  $m/\gamma$  is small, so that we can neglect the acceleration term in (2.2). This is called the *overdamped limit*. Moreover, we

assume that there are no external forces on the particle, set  $\gamma = \sqrt{2\gamma k_B T} = 1$ , and take a one-dimensional space, so that (2.2) reduces to

$$\frac{dX}{dt} = \eta(t). \quad (2.4)$$

We need to integrate this equation to find the trajectory  $X(t)$  that the particle takes. If we assume  $X(0) = 0$ , we find

$$X(t) = \int_0^t \eta(s) ds. \quad (2.5)$$

However, it can be shown that the process  $\eta$  cannot satisfy the properties that would seem reasonable on physical grounds: if we assume that  $\eta(s)$  and  $\eta(t)$  are independent if  $s \neq t$  and that the distribution of  $\eta$  is independent of time, then the process  $\eta$  cannot have continuous sample paths. Moreover, if we require that  $\mathbb{E}[\eta^2] = 1$  then the function  $(t, \omega) \mapsto \eta(t, \omega)$  cannot be measurable with respect to the sigma-algebra  $\mathcal{B}_{[0, \infty]} \times \mathcal{F}$ , with  $\mathcal{B}_{[0, \infty]}$  the Borel sigma-algebra on  $[0, \infty]$  and  $\mathcal{F}$  the sigma algebra on  $\Omega$  [15]. To overcome this problem, we consider the Brownian motion  $B_s$ .

A small increment in Brownian motion  $dB_s$  precisely satisfies the properties that we expect from  $\eta(s) ds$ : its mean is 0, it is continuous and has independent increments. Hence we replace the ‘fluctuating force times a small increment in time  $\eta(s) ds$ ’ by ‘a small increment in Brownian motion  $dB_s$ ’:

$$X_t = \int_0^t dB_s. \quad (2.6)$$

It will not come as a surprise that the integral in Eq. (2.6) evaluates to  $B_t$ , as it should on physical grounds: a particle suspended in a liquid, without any external forces acting on it, performs a Brownian motion.

More generally, we can consider an  $n$ -dimensional equation such as

$$\mathbf{X}_t - \mathbf{X}_0 = \int_0^t \mathbf{b}(s, \mathbf{X}_s) ds + \int_0^t \sigma(s, \mathbf{X}_s) d\mathbf{B}_s, \quad (2.7)$$

where  $\mathbf{b} : \mathbb{R}_+ \times \mathbb{R}^n \rightarrow \mathbb{R}^n$  and  $\sigma : \mathbb{R}_+ \times \mathbb{R}^n \rightarrow \mathbb{R}^{m \times n}$  are given functions, and  $\mathbf{B}_s$  is an  $m$ -dimensional Brownian motion.  $\mathbf{b}$  is called the *drift coefficient* and  $\sigma$  is called the *diffusion coefficient*. (2.7) is usually written as

$$d\mathbf{X}_t = \mathbf{b}(t, \mathbf{X}_t) dt + \sigma(t, \mathbf{X}_t) d\mathbf{B}_t. \quad (2.8)$$

Equations such as this one are called *stochastic differential equations*. The second integral in Eq. (2.7) can however not be interpreted as an ordinary Riemann or Lebesgue integral, but is a so-called *Itô integral*. The rest of this chapter will be devoted to defining this integral and studying its properties.

## 2.3 The Itô integral

First we define the set of functions for which we can define the Itô integral.

**Definition 2.2.** Let  $(\Omega, \mathcal{F}, \mathbb{P})$  be a probability space, and suppose that  $\mathbf{B}_t = (B_1(t), \dots, B_n(t))$  is an  $n$ -dimensional Brownian motion. We write  $V = V(S, T)$ ,  $T > S > 0$ , for the class of functions

$$f : [0, \infty) \times \Omega \rightarrow \mathbb{R} : (t, \omega) \mapsto f(t, \omega) \quad (2.9)$$

such that

1.  $f$  is  $\mathcal{B} \times \mathcal{F}$  measurable,
2. there exists an increasing family of sigma-algebras  $\mathcal{H}_t$ ,  $t \geq 0$  such that
  - (a)  $\mathbf{B}_t$  is a martingale with respect to  $\mathcal{H}_t$  and
  - (b)  $f(t, \cdot)$  is  $\mathcal{H}_t$ -adapted,
3.  $\mathbb{P} \left( \int_S^T f(s, \omega)^2 ds < \infty \right) = 1$ .

Here,  $\mathcal{B}$  is the Borel sigma-algebra, and  $\mathcal{F}_t$  is the sigma-algebra generated by the random variables  $\{B_i(s)\}_{1 \leq i \leq n, 0 \leq s \leq t}$ .

Next we define *elementary functions*, which we will need to approximate arbitrary functions  $f \in V$ .

**Definition 2.3.** A function  $\phi \in V$  is called *elementary* if it is of the form

$$\phi(t, \omega) = \sum_{j=1}^k e_j(\omega) \chi_{[t_{j-1}, t_j)}(t), \quad (2.10)$$

where  $S = t_0 < t_1 < \dots < t_k = T$ , and  $\chi_A$  is the characteristic function of  $A \subset \mathbb{R}$ :

$$\chi_A(t) = \begin{cases} 1 & \text{if } t \in A, \\ 0 & \text{if } t \notin A. \end{cases} \quad (2.11)$$

For arbitrary functions  $f \in V(S, T)$  we will define the Itô integral

$$\int_S^T f(t, \omega) dB_t(\omega) \quad (2.12)$$

by approximating  $f$  by elementary functions. We define the Itô integral of an elementary function  $\phi(t, \omega) = \sum_j e_j(\omega) \chi_{[t_j, t_{j+1})}(t) \in V(S, T)$  as

$$\int_S^T \phi(t, \omega) dB_t(\omega) = \sum_j e_j(\omega) [B_{t_{j+1}} - B_{t_j}](\omega). \quad (2.13)$$

Now we are in a position to define the Itô integral of an arbitrary function  $f \in V$ .

**Definition 2.4.** Let  $f \in V(S, T)$ . Then the *Itô integral* of  $f$  is defined as

$$\int_S^T f(t, \omega) dB_t(\omega) = \lim_{n \rightarrow \infty} \int_S^T \phi_n(t, \omega) dB_t(\omega), \quad (2.14)$$

where the limit is in  $L^2(\mathbb{P})$ . Here  $\{\phi_n\}$  is a sequence of elementary functions such that

$$\mathbb{E} \left[ \int_S^T (f(t, \omega) - \phi_n(t, \omega))^2 dt \right] \rightarrow 0 \text{ as } n \rightarrow \infty. \quad (2.15)$$

We will not go into the details of showing that it is indeed possible to approximate arbitrary  $f$  by elementary functions. From the way the Itô integral is constructed, the *Itô isometry* immediately follows:

**Corollary 2.5.** *Let  $f \in V(S, T)$ . Then*

$$\mathbb{E} \left[ \left( \int_S^T f(t, \omega) dB_t \right)^2 \right] = \mathbb{E} \left[ \int_S^T f^2(t, \omega) dt \right]. \quad (2.16)$$

**Definition 2.6.** Let  $B_t$  be a one-dimensional Brownian motion on  $(\Omega, \mathcal{F}, \mathbb{P})$ . An *Itô process* is a stochastic process  $X_t$  on  $(\Omega, \mathcal{F}, \mathbb{P})$  of the form

$$X_t = X_0 + \int_0^t b(s, X_s) ds + \int_0^t \sigma(s, X_s) dB_s, \quad (2.17)$$

where  $\sigma \in V$ , and  $b$  is  $\mathcal{H}_t$ -adapted and

$$\mathbb{P} \left( \int_0^t |b(s, \omega)| ds < \infty \text{ for all } t \geq 0 \right) = 1. \quad (2.18)$$

An  $n$ -dimensional Itô process is defined analogously; each of the components of the vector- and matrix-valued functions  $\mathbf{b}$  and  $\sigma$  has to satisfy the above conditions.

The following theorem, Itô's formula, provides an easy way to calculate Itô integrals. Similarly to the fundamental theorem of calculus, it allows to compute an integral directly, rather than having to use its cumbersome definition.

**Theorem 2.7.** *Let*

$$d\mathbf{X}(t) = \mathbf{b}(t, \mathbf{X}_t) dt + \sigma(t, \mathbf{X}_t) d\mathbf{B}(t) \quad (2.19)$$

be an  $n$ -dimensional Itô process, with  $\mathbf{b}$  and  $\sigma$  as in Definition 2.6. Let

$$g : [0, \infty) \times \mathbb{R}^n \rightarrow \mathbb{R}^p : (t, \mathbf{x}) \mapsto (g_1(t, \mathbf{x}), \dots, g_p(t, \mathbf{x})), \quad (2.20)$$

and suppose  $g$  is  $C^2$ . Then the process  $\mathbf{Y}_t(\omega) = g(t, \mathbf{X}_t)$  is again an Itô process, whose component  $k = 1, \dots, p$  is given by

$$dY_k(t) = \frac{\partial g_k}{\partial t} dt + \sum_{i=1}^n \frac{\partial g_k}{\partial x_i} dX_i(t) + \frac{1}{2} \sum_{i,j=1}^n \frac{\partial^2 g_k}{\partial x_i \partial x_j} dX_i(t) dX_j(t) \quad (2.21)$$

where  $dB_i dB_j = \delta_{ij} dt$  and  $dt dt = dB_i dt = dt dB_i = 0$ .

The following theorem provides sufficient conditions for SDEs to have a unique solution. We will use this theorem to show that the system we simulate, introduced in the next Chapter, has a unique solution.

**Theorem 2.8.** *Let  $T > 0$  and  $\mathbf{b} : [0, T] \times \mathbb{R}^n \rightarrow \mathbb{R}^n$ ,  $\sigma : [0, T] \times \mathbb{R}^n \rightarrow \mathbb{R}^{n \times m}$  measurable functions satisfying*

$$|\mathbf{b}(t, \mathbf{x})| + |\sigma(t, \mathbf{x})| \leq C(1 + |\mathbf{x}|), \quad \mathbf{x} \in \mathbb{R}^n, t \in [0, T], \quad (2.22)$$

for some  $C > 0$ , with  $|\sigma^2| := \sum |\sigma_{ij}|^2$ , and such that

$$|\mathbf{b}(t, \mathbf{x}) - \mathbf{b}(t, \mathbf{y})| + |\sigma(t, \mathbf{x}) - \sigma(t, \mathbf{y})| \leq D|\mathbf{x} - \mathbf{y}|, \quad \mathbf{x}, \mathbf{y} \in \mathbb{R}^n, t \in [0, T]. \quad (2.23)$$

Let  $\mathbf{Z}$  be a random variable that is independent of the sigma-algebra generated by  $\mathbf{B}_s$ ,  $s \geq 0$ , and such that  $\mathbb{E} [|\mathbf{Z}|^2] < \infty$ . Then the stochastic differential equation

$$d\mathbf{X}_t = \mathbf{b}(t, \mathbf{X}_t) dt + \sigma(t, \mathbf{X}_t) d\mathbf{B}_t, \quad t \in [0, T], \mathbf{X}_0 = \mathbf{Z} \quad (2.24)$$

has a unique  $t$ -continuous solution.

## 2.4 Diffusion processes

**Definition 2.9.** A (time-homogeneous) *Itô diffusion* is a stochastic process  $\mathbf{X}_t(\omega) = \mathbf{X}(t, \omega) : [s, \infty) \times \Omega \rightarrow \mathbb{R}^n$  satisfying a stochastic differential equation of the form

$$d\mathbf{X}_t = \mathbf{b}(\mathbf{X}_t) dt + \sigma(\mathbf{X}_t) d\mathbf{B}_t, \quad t \geq s; \mathbf{X}_s = \mathbf{x}, \quad (2.25)$$

where  $\mathbf{B}_t$  is an  $m$ -dimensional Brownian motion and  $\mathbf{b} : \mathbb{R}^n \rightarrow \mathbb{R}^n$ ,  $\sigma : \mathbb{R}^n \rightarrow \mathbb{R}^{n \times m}$  satisfy, for some  $D \geq 0$  and for all  $\mathbf{x}, \mathbf{y} \in \mathbb{R}^n$

$$|\mathbf{b}(\mathbf{x}) - \mathbf{b}(\mathbf{y})| + |\sigma(\mathbf{x}) - \sigma(\mathbf{y})| \leq D|\mathbf{x} - \mathbf{y}|, \quad (2.26)$$

where  $|\sigma|^2 = \sum |\sigma_{ij}|^2$ .

In particular, the functions  $\mathbf{b}$  and  $\sigma$  are independent of time for an Itô diffusion, and are Lipschitz continuous.

For diffusion processes, we can formulate an associated partial differential equation, whose solution is the probability density of the process as a function of space and time.

**Theorem 2.10.** *Suppose  $p_t$  is the density of the Itô diffusion  $X_t$ . Then  $p_t$  satisfies the forward Kolmogorov equation*

$$\partial_t p_t = \frac{1}{2} \sum_{i=1}^n \sum_{j=1}^n \frac{\partial^2}{\partial x_i \partial x_j} ((\sigma \sigma^\top)_{ij} p_t) - \sum_{i=1}^n \frac{\partial (b_i p_t)}{\partial x_i}. \quad (2.27)$$

In physics literature, the forward Kolmogorov equation is usually called the *Fokker-Planck equation*, which is the terminology that we will use in this report.

## 2.5 An important example

We consider the  $n$ -dimensional trajectory  $\mathbf{X}_t \in \mathbb{R}^n$  of a particle that is submerged in a fluid:

$$d\mathbf{X}_t = \sqrt{2D} d\mathbf{B}_t, \quad (2.28)$$

where  $D > 0$  is called the *diffusion constant*. This equation is easily integrated to give

$$\mathbf{X}_t = \sqrt{2D} \mathbf{B}_t, \quad (2.29)$$

where we assume that  $\mathbf{X}_0 = 0$ . We apply Theorem 2.10 to find the Fokker-Planck equation corresponding to this SDE:

$$\begin{aligned}\partial_t p(\mathbf{x}, t) &= D\Delta p(\mathbf{x}, t), \\ p(\mathbf{x}, 0) &= \delta(\mathbf{x}),\end{aligned}\tag{2.30}$$

where  $p$  is the probability density for the position  $\mathbf{x}$  of the particle at time  $t$ . From this example it becomes clear that Fokker-Planck equations should be interpreted in a generalised sense: to  $p$  there corresponds a linear functional  $T_p : \mathcal{D} \rightarrow \mathbb{R}$ . Here  $\mathcal{D}$  is the space of ‘test’ functions  $\phi : \mathbb{R}^n \rightarrow \mathbb{R}$  that are infinitely often continuously differentiable and have compact support in  $\mathbb{R}^n$ . That is, if  $\phi : \mathbb{R}^n \rightarrow \mathbb{R}$  is such a test function, then

$$T_p(\phi) = \int_{\mathbb{R}^n} p(\mathbf{x}, t)\phi(\mathbf{x}) \, d\mathbf{x}.\tag{2.31}$$

By abuse of notation, we will often write  $p$  instead of  $T_p$ , that is, we will denote the generalised function by its kernel [18].

Equation (2.30) is the *diffusion equation*, whose solution is given by

$$p(\mathbf{x}, t) = \frac{1}{(4\pi Dt)^{n/2}} \exp\left(-\frac{|\mathbf{x}|^2}{4Dt}\right),\tag{2.32}$$

as can easily be verified. Note that we recover (2.1) if we set  $D = 1$ .

Both from symmetry considerations and direct computation, it follows that  $\mathbb{E}[\mathbf{X}_t] = 0$ . The second moment, or *mean squared displacement* (MSD) is more interesting:

$$\mathbb{E}[|\mathbf{X}_t|^2] := \int_{\mathbb{R}^n} |\mathbf{x}|^2 p(\mathbf{x}, t) \, d\mathbf{x} = 2nDt.\tag{2.33}$$

This way we have related the MSD to the diffusion coefficient:  $\text{MSD}(t) = 2nDt$ , an equality known as the *Einstein relation*. This linear behaviour of the MSD is called *normal diffusion*. The situation in which  $\text{MSD}(t) \sim t^\alpha$ ,  $\alpha \neq 1$  is called *anomalous diffusion*.

## 2.6 Active matter

The Brownian motion described in Section 2.5 is that of a single freely diffusing particle in the overdamped limit. However, many (bio-)physical situations are more complicated. In these situations, the MSD is typically not linear in time, and the diffusion is called *anomalous*.

For instance, the particle can propel itself, in which case it is called *active* [1]. Although there are many different ways to model active Brownian particles, we will use the following SDEs to describe their motion in two dimensions (in the overdamped limit):

$$d\mathbf{R}_t = \frac{1}{\gamma} \mathbf{F} \, dt + v \cdot (\cos(\Phi_t), \sin(\Phi_t)) \, dt + \sqrt{2D_T} \, d\mathbf{B}_t,\tag{2.34}$$

$$d\Phi_t = \sqrt{2D_R} \, dW_t.\tag{2.35}$$

Here  $\mathbf{R}_t$  is the particle’s position and  $\Phi_t$  is its angle with respect to the  $x$ -axis.  $\mathbf{B}_t$  and  $W_t$  are two- and one-dimensional Brownian motions with diffusion

coefficients  $D_T$  and  $D_R$  respectively.  $\mathbf{F}$  is some deterministic force, coming e.g. from interactions with other particles, and  $v$  is the constant magnitude of the velocity with which the particle propels itself. Hence, not only the position of the particle diffuses, but also its angle. Active Brownian particles travel much faster than passive ones, as follows from the following theorem.

**Theorem 2.11.** *Consider the SDEs*

$$d\mathbf{R}_t = v \cdot (\cos \Phi_t, \sin \Phi_t) dt + \sigma d\mathbf{B}_t \quad (2.36a)$$

$$d\Phi_t = \nu dW_t, \quad (2.36b)$$

with initial conditions  $\mathbf{R}_0 = 0$  and  $\Phi_0 = 0$ .  $\mathbf{B}_t$  and  $W_t$  are two- and one-dimensional independent Brownian motions respectively, and  $v$ ,  $\sigma$  and  $\nu$  are positive constants. Then the MSD of  $\mathbf{R}_t$  is given by

$$\text{MSD}(t) = \mathbb{E} [|\mathbf{R}_t|^2] = \left(2\sigma^2 + \frac{4v^2}{\nu^2}\right) t + \frac{8v^2}{\nu^4} \left(\exp\left(-\frac{t\nu^2}{2}\right) - 1\right). \quad (2.37)$$

In the proof of this theorem, we will use the following lemma.

**Lemma 2.12.** *Let  $W_t$  be a Brownian motion with  $W_0 \in \mathbb{R}$  given, let  $\nu > 0$ . Then*

$$\mathbb{E}[\cos(\nu W_t)] = \exp\left(-\frac{t\nu^2}{2}\right) \cos(\nu W_0), \quad (2.38a)$$

$$\mathbb{E}[\sin(\nu W_t)] = \exp\left(-\frac{t\nu^2}{2}\right) \sin(\nu W_0). \quad (2.38b)$$

*Proof.* We first consider the case  $W_0 = 0$ . Let  $V_t$  be a Brownian motion such that  $V_0 = 0$ . We use the power series of the cosine:

$$\mathbb{E}[\cos(\nu V_t)] = \mathbb{E}\left[\sum_{n=0}^{\infty} (-1)^n \frac{(\nu V_t)^{2n}}{(2n)!}\right]. \quad (2.39)$$

By the dominated convergence theorem, we can interchange summation and expectation:

$$\mathbb{E}\left[\sum_{n=0}^{\infty} (-1)^n \frac{(\nu V_t)^{2n}}{(2n)!}\right] = \sum_{n=0}^{\infty} \frac{(-1)^n}{(2n)!} \nu^{2n} \mathbb{E}[V_t^{2n}] \quad (2.40)$$

The even moments of the normally distributed random variable  $V_t$  are

$$\mathbb{E}[V_t^{2n}] = \frac{(2n)!}{2^n n!} t^n. \quad (2.41)$$

Hence

$$\mathbb{E}[\cos(\nu V_t)] = \sum_{n=0}^{\infty} \left(-\frac{t\nu^2}{2}\right)^n \frac{1}{n!} = \exp\left(-\frac{t\nu^2}{2}\right), \quad (2.42)$$

by the power series for the exponential. The proof for  $\mathbb{E}[\sin(\nu V_t)] = 0$  follows from the fact that the sine is an odd function and the distribution of  $V_t$  is even.

Now, since  $W_0 \neq 0$  in general, we write  $W_t = V_t + W_0$ . Application of a trigonometric angle sum identity yields

$$\mathbb{E}[\cos(\nu W_t)] = \mathbb{E}[\cos(\nu V_t) \cos(\nu W_0)] - \mathbb{E}[\sin(\nu V_t) \sin(\nu W_0)], \quad (2.43)$$

$$= \exp\left(-\frac{t\nu^2}{2}\right) \cos(\nu W_0), \quad (2.44)$$

where we have used independence of  $V_t$  and  $W_0$ , and that  $\mathbb{E}[\sin(\nu V_t)] = 0$ . Similarly,

$$\mathbb{E}[\sin(\nu W_t)] = \exp\left(-\frac{t\nu^2}{2}\right) \sin(\nu W_0). \quad (2.45)$$

□

*Proof of Theorem 2.11.* First we define the vector

$$\mathbf{Y}_t := (Y_1(t), Y_2(t)) := (\cos \Phi_t, \sin \Phi_t) = (\cos(\nu W_t), \sin(\nu W_t)). \quad (2.46)$$

$\mathbf{Y}_t$  satisfies the SDE

$$d\mathbf{Y}_t = -\frac{\nu^2}{2} \mathbf{Y}_t dt + \nu K \mathbf{Y}_t dW_t \quad (2.47)$$

where  $K$  is the matrix

$$K = \begin{pmatrix} 0 & -1 \\ 1 & 0 \end{pmatrix}. \quad (2.48)$$

This follows from the application of Itô's formula. Integrating and squaring the SDE (2.36a) yields

$$|\mathbf{R}_t|^2 = v^2 \left| \int_0^t \mathbf{Y}_t dt \right|^2 + \sigma \mathbf{B}_t \cdot \int_0^t \mathbf{Y}_t dt + \sigma^2 |\mathbf{B}_t|^2. \quad (2.49)$$

We take the expectation value on both sides to find the MSD:

$$\begin{aligned} \text{MSD}(t) := \mathbb{E} [|\mathbf{R}_t|^2] &= v^2 \mathbb{E} \left[ \left| \int_0^t \mathbf{Y}_t dt \right|^2 \right] \\ &+ \mathbb{E} \left[ \sigma \mathbf{B}_t \cdot \int_0^t \mathbf{Y}_t dt \right] + \sigma^2 \mathbb{E} [|\mathbf{B}_t|^2]. \end{aligned} \quad (2.50)$$

For the last term in this equation we simply have

$$\mathbb{E} [|\mathbf{B}_t|^2] = \mathbb{E} [B_1(t)^2 + B_2(t)^2] = 2t \quad (2.51)$$

since  $B_1(t)$  and  $B_2(t)$  are independent Brownian motions. Moreover, by independence of  $\mathbf{B}_t$  and  $W_t$ , we have

$$\mathbb{E} \left[ \sigma \mathbf{B}_t \cdot \int_0^t \mathbf{Y}_t dt \right] = \sigma \mathbb{E} [\mathbf{B}_t] \cdot \mathbb{E} \left[ \int_0^t \mathbf{Y}_t dt \right] = 0, \quad (2.52)$$

since  $\mathbb{E} [\mathbf{B}_t] = 0$ .



To evaluate the first integral in (2.50) we use our observation about  $\mathbf{Y}_t$ :

$$\cos(\nu W_t) dt = -\frac{2}{\nu} \sin(\nu W_t) dW_t - \frac{2}{\nu^2} d \cos(\nu W_t) \quad (2.53a)$$

$$\sin(\nu W_t) dt = \frac{2}{\nu} \cos(\nu W_t) dW_t - \frac{2}{\nu^2} d \sin(\nu W_t). \quad (2.53b)$$

Hence

$$\int_0^t \cos(\nu W_t) dt = -\frac{2}{\nu} \int_0^t \sin(\nu W_t) dW_t - \frac{2}{\nu^2} (\cos(\nu W_t) - 1), \quad (2.54a)$$

$$\int_0^t \sin(\nu W_t) dt = \frac{2}{\nu} \int_0^t \cos(\nu W_t) dW_t - \frac{2}{\nu^2} \sin(\nu W_t). \quad (2.54b)$$

Squaring these two equations, taking their expectations and summing them yields

$$\begin{aligned} \frac{1}{4} \mathbb{E} \left[ \left( \int_0^t \mathbf{Y}_t^2 dt \right)^2 \right] &= \frac{1}{\nu^2} \mathbb{E} \left[ \left( \int_0^t \sin(\nu W_s) dW_s \right)^2 \right] \\ &+ \frac{2}{\nu^3} \mathbb{E} \left[ (\cos(\nu W_t) - 1) \int_0^t \sin(\nu W_s) dW_s \right] + \frac{1}{\nu^4} \mathbb{E} [(\cos(\nu W_t) - 1)^2] \\ &+ \frac{1}{\nu^2} \mathbb{E} \left[ \left( \int_0^t \cos(\nu W_s) dW_s \right)^2 \right] - \frac{2}{\nu^3} \mathbb{E} \left[ \sin(\nu W_s) \int_0^t \cos(\nu W_s) dW_s \right] \\ &+ \frac{1}{\nu^4} \mathbb{E} [\sin^2(\nu W_t)]. \end{aligned} \quad (2.55)$$

Hence we now have six expectations on the right-hand side that we need to evaluate. To the first term we apply the Itô isometry:

$$\mathbb{E} \left[ \left( \int_0^t \sin(\nu W_s) dW_s \right)^2 \right] = \mathbb{E} \left[ \int_0^t \sin^2(\nu W_s) ds \right], \quad (2.56)$$

and similarly for the fourth term, so that

$$\mathbb{E} \left[ \left( \int_0^t \sin(\nu W_s) dW_t \right)^2 \right] + \mathbb{E} \left[ \left( \int_0^t \cos(\nu W_s) dW_s \right)^2 \right] = \mathbb{E} \left[ \int_0^t 1 ds \right] = t, \quad (2.57)$$

using linearity of expectation and integration and the fact that  $\sin^2(\nu W_t) + \cos^2(\nu W_t) = 1$ .

Next we consider the second term. We have

$$\begin{aligned} \mathbb{E} \left[ \cos(\nu W_t) \int_0^t \sin(\nu W_s) ds \right] &= \frac{1}{\nu} \mathbb{E} [\cos(\nu W_t)] - \frac{1}{\nu} \mathbb{E} [\cos^2(\nu W_t)] \\ &- \frac{\nu}{2} \mathbb{E} \left[ \int_0^t \cos(\nu W_t) \cos(\nu W_s) ds \right], \end{aligned} \quad (2.58)$$

which follows from (2.54a). If we interchange the expectation operator and the integral, use a trigonometric relationship and Lemma 2.12 we can write

$$\begin{aligned} \mathbb{E} \left[ \cos(\nu W_t) \int_0^t \sin(\nu W_s) ds \right] &= \frac{1}{\nu} \exp \left( -\frac{t\nu^2}{2} \right) - \frac{1}{\nu} \mathbb{E} [\cos^2(\nu W_t)] \\ &- \frac{\nu}{4} \int_0^t \left[ \exp \left( -\frac{(t-s)\nu^2}{2} \right) + \exp \left( -\frac{(t+s)\nu^2}{2} \right) \right] ds, \end{aligned} \quad (2.59)$$

which equals

$$\frac{1}{\nu} \exp\left(-\frac{t\nu^2}{2}\right) - \frac{1}{\nu} \mathbb{E}[\cos^2(\nu W_t)] - \frac{1}{2\nu} (1 - \exp(t\nu^2)). \quad (2.60)$$

Similarly, we find that

$$\begin{aligned} \mathbb{E}\left[\sin(\nu W_t) \int_0^t \cos(\nu W_s) dW_s\right] &= \frac{1}{\nu} \mathbb{E}[\sin^2(\nu W_t)] \\ &+ \frac{1}{2\nu} \left(1 - 2 \exp\left(-\frac{t\nu^2}{2}\right) + \exp(-t\nu^2)\right). \end{aligned} \quad (2.61)$$

If we substitute these results in (2.55), we find

$$\frac{1}{4} \mathbb{E}\left[\left|\int_0^t \mathbf{Y}_t^2 dt\right|^2\right] = \frac{t}{\nu^2} + \frac{2}{\nu^2} \left(\exp\left(-\frac{t\nu^2}{2}\right) - 1\right). \quad (2.62)$$

Hence

$$\text{MSD}(t) = \mathbb{E}\left[|\mathbf{R}_t|^2\right] = \left(2\sigma^2 + \frac{4v^2}{\nu^2}\right)t + \frac{8v^2}{\nu^4} \left(\exp\left(-\frac{t\nu^2}{2}\right) - 1\right). \quad (2.63)$$

□

In physics literature, one usually sees the choices

$$\sigma = \sqrt{2D_T} \quad \text{and} \quad \nu = \sqrt{2D_R}, \quad (2.64)$$

with  $D_T$  and  $D_R$  the translational and rotational diffusion coefficients, respectively. Then the expression for the MSD becomes

$$\text{MSD}(t) = \left(4D_T + \frac{2v^2}{D_R}\right)t + \frac{2v^2}{D_R^2} (\exp(-tD_R) - 1), \quad (2.65)$$

as is found in literature [1]. If  $t$  is small, we can Taylor expand the exponential term, to find

$$\text{MSD}(t) \approx 4D_T t + v^2 t^2. \quad (2.66)$$

Hence, for very small  $t$  the MSD is linear in  $t$ , and  $\text{MSD}(t) \sim t^2$  for  $t \gg 4D_T/v^2$ , but still small (if  $v$  is too small or  $D_T$  is too large this ballistic regime will not be observed). As  $t \rightarrow \infty$ , the exponential term vanishes and  $\text{MSD}(t) \sim t$  again.

# Chapter 3

## Model description

### 3.1 Model

We consider the movement of a big, passive Brownian particle in a bath of small, active Brownian particles. All these particles are suspended in a liquid. The big particle is called the *tracer*, whereas the small particles are called *host* particles. We model the active particles with the Kob-Andersen-Lennard-Jones (KALJ) model [19], which means the following. The bath of host particles is modelled as a binary mixture of particles of type A and B. 65% of the host particles are of type A; the remaining 35% are of type B. The particles live in a two-dimensional rectangular domain  $\Omega \subset \mathbb{R}^2$ . We use periodic boundary conditions. Without the presence of the tracer and neglecting inertia, the (overdamped) Langevin equations for the  $N$  host particles are

$$\begin{aligned}\gamma d\mathbf{R}_t^i &= (-\nabla_{\mathbf{r}_i} U^i + \gamma \mathbf{v}^i) dt + \sqrt{2}\gamma\sigma d\mathbf{B}_t^i, \\ \gamma_R d\Phi_t^i &= \sqrt{2}\gamma_R\nu dW_t^i.\end{aligned}\tag{3.1}$$

Here  $\mathbf{R}_t^i = (X_t^i, Y_t^i) \in \Omega$  is the position of the  $i$ th particle at time  $t$ ,  $i \in \{1, \dots, N\}$ , and  $\Phi_t^i$  is its orientation.  $U^i : \mathbb{R}^{2N} \rightarrow \mathbb{R}$  is its interaction potential, that in general depends on the positions of all particles in the system.  $\nabla_{\mathbf{r}_i}$  denotes differentiation with respect to the position coordinate of the  $i$ th particle. The activity of the particles is described by the active velocity vector  $\mathbf{v}^i = v_0(\cos \Phi_t^i, \sin \Phi_t^i)$ , with constant magnitude  $v_0$ . The translational and rotational diffusivity are specified by  $\sigma$  and  $\nu$  respectively, and  $\gamma$  and  $\gamma_R$  are the translational and rotational friction coefficients respectively. We have the following relations:

$$\sigma = \sqrt{D_T} \text{ and } \nu = \sqrt{D_R},\tag{3.2}$$

with  $D_T$  and  $D_R$  being the translational and rotational diffusion coefficients respectively. Moreover,  $\mathbf{B}_t^i = (B_{x,t}^i, B_{y,t}^i)$  is a two-dimensional Brownian motion, and  $W_t^i$  is a one-dimensional Brownian motion that causes the fluctuations in the orientation of the particles. Hence we need a set of  $3N$  stochastic differential equations to describe the behaviour of the host particles. We neglect hydrodynamic interactions, which is reasonable since the environment is highly crowded [1, 14].

The interaction potential  $U^i$  of particle  $i$  is the sum of the interaction potentials of particle  $i$  with particle  $j \neq i$ :

$$U^i = \sum_{j \neq i} u_{ij}(\mathbf{r}_i - \mathbf{r}_j). \quad (3.3)$$

For these two-particle interaction potentials  $u_{ij}$  we use the Weeks-Chandler-Andersen potential, which is a truncated and shifted Lennard-Jones potential: if  $\mathbf{r}$  is the difference in position between two particles  $i$  and  $j$  and  $r = |\mathbf{r}|$ , then

$$u_{ij}(\mathbf{r}) = \begin{cases} 4\varepsilon_{ij} \left[ \left( \frac{\sigma_{ij}}{r} \right)^{12} - \left( \frac{\sigma_{ij}}{r} \right)^6 \right] + \varepsilon_{ij}, & \text{if } r < r_c \\ 0, & \text{if } r \geq r_c, \end{cases} \quad (3.4)$$

with  $r_c = 2^{1/6}\sigma_{ij}$ . Hence we only maintain the repulsive part of the Lennard-Jones potential. The shift  $+\varepsilon_{ij}$  is only for differentiability purposes. The values of the parameters  $\varepsilon_{ij}$  and  $\sigma_{ij}$  depend on the type of particle: in the numerical simulations we set  $\varepsilon_{AA} = 1.0$ ,  $\sigma_{AA} = 1.0$ ,  $\varepsilon_{AB} = 1.5$ ,  $\sigma_{AB} = 0.8$ ,  $\varepsilon_{BB} = 0.5$  and  $\sigma_{BB} = 0.88$ . These values are chosen as it is known that they prevent crystallisation of the system [20].

These equations (3.1) have to be adjusted in order to incorporate the tracer as well and to describe the interaction of the tracer with its environment and vice versa. This tracer has the same diffusivity as the hosts, but is passive and is much larger. We also describe its motion by an overdamped Langevin equation. We add to (3.1) the following equation for the tracer's position  $\mathbf{Z}_t$ :

$$d\mathbf{Z}_t = -\nabla_{\mathbf{z}} U^T dt + \sqrt{2}\sigma d\mathbf{B}_t^T. \quad (3.5)$$

Since the tracer is passive there is no need to describe its angle. Here  $U^T : \mathbb{R}^{2(N+1)} \rightarrow \mathbb{R}$  represents the interaction of the tracer with its environment,

$$U^T = \sum_{i=1}^N u_{Ti}(\mathbf{z} - \mathbf{r}_i), \quad (3.6)$$

where  $u_{Ti}$  again is a WCA potential, with  $\varepsilon_{TA} = \varepsilon_{TB} = 1.0$ ,  $\sigma_{TA} = 3 + \sigma_{AA}/2$ ,  $\sigma_{TB} = 3 + \sigma_{BB}/2$ . The potentials in (3.1) are modified as follows:

$$U^i = \sum_{j \neq i} u_{ij}(\mathbf{r}_i - \mathbf{r}_j) + u_{iT}(\mathbf{r}_i - \mathbf{z}). \quad (3.7)$$

Overall, the system is described by the following system of equations for particle  $i = 1, \dots, N$ :

$$d\mathbf{R}_t^i = \left[ -\frac{1}{\gamma} \left( \nabla_{\mathbf{r}_i} \sum_{j \neq i} u_{ij}(\mathbf{R}_t^i - \mathbf{R}_t^j) + \nabla_{\mathbf{r}_i} u_{iT}(\mathbf{R}_t^i - \mathbf{Z}) \right) + v_0 (\cos(\Phi_t^i), \sin(\Phi_t^i)) \right] dt + \sqrt{2}\sigma d\mathbf{B}_t, \quad (3.8a)$$

$$d\Phi_t^i = \sqrt{2}\nu dW_t^i, \quad (3.8b)$$

and the tracer's dynamics are governed by the SDEs

$$d\mathbf{Z} = -\frac{1}{\gamma}\nabla_{\mathbf{z}}\sum_{j=1}^N u_{Tj}(\mathbf{Z}_t - \mathbf{R}_t^j)dt + \sqrt{2}\sigma d\mathbf{B}_t^T. \quad (3.8c)$$

The number density is  $\rho = N/V$ , with  $V$  the area of the domain  $\Omega$ . We define the dimensionless density  $\rho^* = \sigma_{AA}^2\rho$ . Moreover, we define the dimensionless temperature  $T^* = k_B T/\varepsilon_{AA}$ , and the dimensionless time  $t^* = t(\varepsilon_{AA}/\gamma\sigma^2)$ . The dimensionless density is related to the area fraction  $f$  by  $f = \frac{\pi}{4}\rho^*$ .

## 3.2 Brownian dynamics simulations

We take  $N$  host particles and a density  $\rho$ , so that the box length is  $L = \sqrt{N/\rho}$ . To initialise the system, we place the tracer on  $(2^{1/6}\sigma_{AT}, 2^{1/6}\sigma_{AT})$ , and place the hosts in the set  $[2 \cdot 2^{1/6}\sigma_{AT}, L']^2$ , where  $L' := \lceil(1 + 2^{1/6}\sigma_{AA}/2)\sqrt{N+1}\rceil$ . The A and B particles are randomly placed on a square lattice of  $\lceil\sqrt{N}\rceil^2$  points. (Some of these points remain unoccupied if  $N < \lceil\sqrt{N}\rceil^2$ .) This way we make sure that the particles (neither the tracer nor the hosts) can be too close or even overlap. We then shrink the box from  $[0, L']^2$  to  $[0, L]^2$  in  $2 \cdot 10^5$  time steps, of size  $\Delta t = 10^{-5}$ . When we take  $\Delta t$  one order of magnitude larger, the particle's displacements incidentally may become larger than 1.

Rather than numerically integrating the SDE that governs the diffusion of the angle  $\phi$  of an active particle, we directly integrate the unit vector  $\hat{\mathbf{v}} := (v_x, v_y)$  that determines its orientation:

$$v'_x|_{t+\Delta t} = v_x|_t + \sqrt{2D_R\Delta t}v_y|_t\eta, \quad \text{and} \quad v'_y|_{t+\Delta t} = v_y|_t - \sqrt{2D_R\Delta t}v_x|_t\eta, \quad (3.9)$$

where  $\eta \sim \mathcal{N}(0, 1)$ . The unit vector  $(v_x, v_y)|_{t+\Delta t}$  is then obtained by normalising  $(v'_x, v'_y)|_{t+\Delta t}$ . Initially, both components of the orientation vector are uniformly distributed on the interval  $[-1, 1]$ .

The SDEs that describe the particle's position are integrated using the Euler-Maruyama method [21]. If  $\mathbf{R}_i$  is the position of either the host or the tracer, we have (in case of the tracer we take  $v_0 = 0$ )

$$\mathbf{R}_i|_{t+\Delta t} = \mathbf{R}_i|_t + \frac{1}{\gamma}\mathbf{f}\Delta t + v_0(v_x, v_y)|_t + \sqrt{2D_T\Delta t}\xi \quad (3.10)$$

where  $\xi = (\xi_x, \xi_y)$ , with  $\xi_x, \xi_y \sim \mathcal{N}(0, 1)$ , and

$$\mathbf{f} = -\sum_{j \neq i} \frac{\partial u_{ij}(r)}{\partial r} \Big|_{R_{ij}} \frac{\mathbf{R}_{ij}}{R_{ij}} \quad (3.11)$$

is the interaction force between particle  $i$  and all other particles.  $\mathbf{R}_{ij}$  denotes the distance between particle  $i$  and  $j$ . Note that  $\sqrt{\Delta t}\xi_x \sim \mathcal{N}(0, \Delta t)$ , which is in agreement with  $B_t - B_s \sim \mathcal{N}(0, t - s)$ . For computational efficiency, we divide the box into  $\lfloor L/(2^{1/6}\sigma_{AA} + 1) \rfloor^2$  square cells. Each particle, except the tracer, is placed in one of these cells, according to the particle's position. We only calculate the interaction force between particle  $i \in \{1, \dots, N\}$  and the particles in the same cell, and between  $i$  and all particles in the eight cells

that directly surround particle  $i$ 's cell. This way, we do not need to check the distance between  $i$  and all other particles. However for the tracer, we calculate its interaction with *all* of the hosts, as the tracer's range of interaction is much larger than that of the hosts.

We set  $\gamma = \gamma_R = 1$  and  $D_T = D_R = T$ , and we take  $N = 500$  particles. The number density  $\rho$ , temperature  $T$  and velocity  $v_0$  are varied. For the density  $\rho$  we take the values 0.1, 0.5 and 0.8, corresponding to area fractions  $f$  of approximately 0.079, 0.393 and 0.628 respectively. The temperature is always chosen between 0.5 and 5; for most runs  $T = 1, 2$  or 5. Both the lower and the upper bound on  $T$  are chosen for efficiency; for lower temperatures the system needs longer to equilibrate, whereas for  $T > 5$  the particle displacements become too large at the time step size that we use. The velocity  $v_0$  ranges from 0 to 50. We should stress that the effect of temperature or velocity on the MSD is not our main interest; we will rather look at the nondimensionalised ratio  $v_0/T$ . Clearly, temperatures that differ by one order of magnitude are unphysical in the sense that the supporting liquid will not be liquid on the entire temperature range.

After the box has shrunk to the desired size, we let the system reach a steady state for  $2 \cdot 10^7$  time steps. For each choice of variables  $T$ ,  $v_0$  and  $\rho$  we run two simulations: one with a simulation time of  $t = 20$ , of which we save each tenth time step, and one with a simulation time of  $t = 500$ , of which we save each 1000th time step. The first of these two simulations is used to analyse the short and intermediate time diffusion, whereas the latter is used to analyse the long-time diffusion. For each choice of  $T$ ,  $v_0$  and  $\rho$  we run 25 simulations with different initial conditions.

The tracer's MSD is defined as

$$\text{MSD}(t) = \mathbb{E} \left[ |\mathbf{Z}_t - \mathbf{Z}_0|^2 \right]. \quad (3.12)$$

Because of the periodic boundary conditions, we set for the  $x$ -component of the tracer's position  $\mathbf{Z}_t = (X_t, Y_t)$ , for  $k$  between 0 and the number of time steps

$$X_{|k\Delta t}^{\text{new}} = X_{|k\Delta t}^{\text{old}} - \left\lfloor \frac{X_{|k\Delta t}^{\text{old}} - X_{|(k-1)\Delta t}^{\text{old}}}{L} \right\rfloor L, \quad (3.13)$$

directly after which we set

$$X_{|k\Delta t}^{\text{old}} = X_{|k\Delta t}^{\text{new}}. \quad (3.14)$$

This method is applied iteratively, starting at  $k = 0$ . Hence, when the term  $\left\lfloor (X_{|k\Delta t}^{\text{old}} - X_{|(k-1)\Delta t}^{\text{old}})/L \right\rfloor$  is nonzero, we assume that the tracer has teleported to the other side of the box. We adjust this by adding or subtracting the corresponding number of box lengths from the tracer's coordinate. The same procedure is applied to the  $y$ -component of the tracer's position.

To calculate the tracer's MSD, we take both ensemble and time averages. For the time averages, the maximum correlation time is half the simulation time, and we use each tenth data point as a time origin, so that each point on the MSD profile is averaged over a large number of data points. This procedure is only possible if the system has reached steady state. In order to make sure that this is indeed the case after the equilibration time, we divide the simulation time

$t$  in two intervals  $[0, t/2)$  and  $[t/2, t]$  of equal length. We calculate two MSDs (both as a function of time): one from the positions that the tracer attained during the first interval, and one from the positions that the tracer attained during the second interval. If these two MSDs are equal at each time step, we know that the system has reached steady state. Moreover, we also calculate the MSD of the hosts for these two intervals and again verify whether the MSDs calculated with the different intervals are equal.

## Chapter 4

# Analytical Approximation of the MSD

In this chapter we analytically derive an expression for the MSD of the passive tracer, using a series of approximations. The first approximation is that we assume that all bath particles are of type A, i.e. the active bath consists of only a single type of particle. Therefore, the active particles are indistinguishable. In theory this can result in a crystallisation of the system, but due to the inevitable further simplifications this will not pose a problem.

In Section 4.1, we convert the SDEs for the positions and orientations of the particles to PDEs describing their probability distribution (Theorem 4.4). We integrate this equation over the phase space of the host particles to obtain a PDE for the tracer's marginal density function (Equation (4.39)). Theorem 4.5 states that this PDE depends on the marginal density function of a single host particle that knows the tracer's location. Hence, in Section 4.2, we approximate, largely on physical grounds, this density function. Equation (4.51) gives the approximate expression for this density function. Subsequently, in Section 4.3 we use this result to find an expression for the tracer's MSD, which is given in Theorem 4.10. Eventually, we find that  $\text{MSD}(t) \sim t$  for small  $t$  and  $\text{MSD} \sim t^2$  for large  $t$ . A possible method to improve the approximate expression for the tracer's MSD is outlined in Section 4.4.

### 4.1 Probability density of the tracer

We start by writing the Fokker-Planck equation corresponding to the system with only one type of host particle. However, since the potential energy is singular at  $(0, 0) \in \mathbb{R}^2$ , Theorem 2.10 does not apply: the gradient of such a potential energy function cannot be Lipschitz continuous. Hence, we slightly adapt the potential energy functions: let  $0 < \delta < 2^{1/6}\sigma_{AA}$  and small, and define

$$\tilde{u}_{ij}(\mathbf{r}) := \begin{cases} ar^3 + br^2 + c & \text{if } r < \delta \\ u_{ij}(\mathbf{r}) & \text{else,} \end{cases} \quad (4.1)$$

where  $r := |\mathbf{r}|$ , and where  $a$ ,  $b$  and  $c$  are constants chosen such that  $\tilde{u}_{ij}$  is twice continuously differentiable at  $r = \delta$ .



**Lemma 4.1.** *The gradient of this potential energy function  $\nabla\tilde{u}_{ij}$  is indeed Lipschitz continuous.*

*Proof.* Let  $\mathbf{r} = (x, y), \mathbf{r}' = (x', y') \in \mathbb{R}^2$ , and define  $|\mathbf{r}| = r, |\mathbf{r}'| = r'$ . We make a case distinction:

- $r, r' \leq r_c$ . Define  $\tilde{w}_{ij} : \mathbb{R}_{\geq 0} \rightarrow \mathbb{R}$ ,

$$\tilde{w}_{ij}(r) = \tilde{u}_{ij}(\mathbf{r}), \quad \text{where } r = |\mathbf{r}|. \quad (4.2)$$

Since  $\tilde{u}_{ij}$  only depends on  $\mathbf{r}$  through its length  $r$ ,  $\tilde{w}_{ij}$  is well-defined. Then we have, with  $\hat{\mathbf{r}} := \mathbf{r}/r$ ,

$$|\nabla\tilde{u}_{ij}(\mathbf{r}) - \nabla\tilde{u}_{ij}(\mathbf{r}')| = |\partial_r\tilde{w}_{ij}(r)\hat{\mathbf{r}} - \partial_r\tilde{w}_{ij}(r')\hat{\mathbf{r}}'| \quad (4.3)$$

$$\leq 2|\partial_r\tilde{w}_{ij}(r) - \partial_r\tilde{w}_{ij}(r')| \quad (4.4)$$

$$\leq M_1|r - r'| \leq M_1|\mathbf{r} - \mathbf{r}'|, \quad (4.5)$$

where the second inequality is obtained by the mean value theorem and the fact that the derivative of  $\partial_r\tilde{w}_{ij}$  is bounded by  $M_1$  (on  $[0, 2^{1/6}\sigma_{ij}]$ ). The third inequality follows from the reverse triangle inequality.

- $r < r_c, r' \geq r_c$ . Define  $M_2 := \frac{1}{2} \max_{\rho \in \mathbb{R}_{\geq 0} \setminus \{r_c\}} |\partial_r^2\tilde{w}_{ij}(\rho)|$ . Then

$$|\nabla\tilde{u}_{ij}(\mathbf{r}) - \nabla\tilde{u}_{ij}(\mathbf{r}')| = |\partial_r\tilde{w}_{ij}(r)\hat{\mathbf{r}} - \partial_r\tilde{w}_{ij}(r')\hat{\mathbf{r}}'| \quad (4.6)$$

$$\leq 2|\partial_r\tilde{w}_{ij}(r) - \partial_r\tilde{w}_{ij}(r')| \quad (4.7)$$

$$\leq 2(|\partial_r\tilde{w}_{ij}(r) - \partial_r\tilde{w}_{ij}(r_c)| + |\partial_r\tilde{w}_{ij}(r_c) - \partial_r\tilde{w}_{ij}(r')|) \quad (4.8)$$

Then, again by the mean value theorem, and the reverse triangle inequality

$$|\nabla\tilde{u}_{ij}(\mathbf{r}) - \nabla\tilde{u}_{ij}(\mathbf{r}')| \leq M_2(|r - r_c| + |r_c - r'|) \quad (4.9)$$

$$= M_2|r - r'| \leq M_2|\mathbf{r} - \mathbf{r}'|. \quad (4.10)$$

- $r, r' > r_c$ . Trivial.

Hence  $\nabla\tilde{u}_{ij}$  is Lipschitz with constant  $\max\{M_1, M_2\}$ .  $\square$

However, all terms in the SDEs that describe the motion involve sums of terms like  $\nabla\tilde{u}_{ij}(\mathbf{r}_i - \mathbf{r}_j)$ . The following Lemma establishes that these terms also are Lipschitz, when it is known that  $\nabla\tilde{u}_{ij}$  is Lipschitz. It is easily generalised to sums of arbitrary (finite) length.

**Lemma 4.2.** *Let  $A \subset \mathbb{R}^n$ , and suppose  $f : A \rightarrow \mathbb{R}$  is  $M$ -Lipschitz. Define  $F : A^3 \rightarrow \mathbb{R} : (\mathbf{x}, \mathbf{y}, \mathbf{z}) \mapsto f(\mathbf{x} - \mathbf{y}) + f(\mathbf{x} - \mathbf{z})$ . Then  $F$  is also Lipschitz.*

*Proof.* Let  $(\mathbf{x}, \mathbf{y}, \mathbf{z}), (\mathbf{x}', \mathbf{y}', \mathbf{z}') \in A^3$ . Then, since  $f$  is  $M$ -Lipschitz and by the triangle inequality

$$|F(\mathbf{x}, \mathbf{y}, \mathbf{z}) - F(\mathbf{x}', \mathbf{y}', \mathbf{z}')| \leq |f(\mathbf{x} - \mathbf{y}) - f(\mathbf{x}' - \mathbf{y}')| + |f(\mathbf{x} - \mathbf{z}) - f(\mathbf{x}' - \mathbf{z}')| \quad (4.11)$$

$$\leq M(|\mathbf{x} - \mathbf{y} - \mathbf{x}' + \mathbf{y}'| + |\mathbf{x} - \mathbf{z} - \mathbf{x}' + \mathbf{z}'|) \quad (4.12)$$

$$\leq M(|\mathbf{x} - \mathbf{x}'| + |\mathbf{y} - \mathbf{y}'| + |\mathbf{x} - \mathbf{x}'| + |\mathbf{z} - \mathbf{z}'|) \quad (4.13)$$

Now, if we interpret  $|\mathbf{a}_1| + |\mathbf{a}_2|$  as a norm  $|\mathbf{a}|_0$  of the vector  $\mathbf{a} = (\mathbf{a}_1, \mathbf{a}_2) \in \mathbb{R}^{2n}$ , we have that

$$|\mathbf{a}|_0 \leq c|\mathbf{a}| = c\sqrt{|\mathbf{a}_1|^2 + |\mathbf{a}_2|^2}, \quad (4.14)$$

for some  $c > 0$ , since on a finite-dimensional vector space all norms are equivalent. It follows that there exists  $\tilde{M}$  such that

$$|F(\mathbf{x}, \mathbf{y}, \mathbf{z}) - F(\mathbf{x}', \mathbf{y}', \mathbf{z}')| \leq \tilde{M} \left( \sqrt{|\mathbf{x} - \mathbf{x}'|^2 + |\mathbf{y} - \mathbf{y}'|^2} + \sqrt{|\mathbf{x} - \mathbf{x}'|^2 + |\mathbf{z} - \mathbf{z}'|^2} \right). \quad (4.15)$$

It can be shown that the quantity on the right-hand side is a norm of the vector  $(\mathbf{x} - \mathbf{x}', \mathbf{y} - \mathbf{y}', \mathbf{z} - \mathbf{z}') \in \mathbb{R}^{3n}$ . This norm is equivalent to the Euclidean norm on  $\mathbb{R}^{3n}$ . Hence there exists  $L > 0$  such that

$$|F(\mathbf{x}, \mathbf{y}, \mathbf{z}) - F(\mathbf{x}', \mathbf{y}', \mathbf{z}')| \leq L|(\mathbf{x}, \mathbf{y}, \mathbf{z}) - (\mathbf{x}', \mathbf{y}', \mathbf{z}')|. \quad (4.16)$$

□

**Theorem 4.3.** *A solution to the system (3.8), with initial positions and angles given, and with  $u_{ij}$  replaced by  $\tilde{u}_{ij}$  exists and is unique.*

*Proof.* We apply Theorem 2.8. The  $i$ th component of the  $(3N + 2)$ -dimensional ‘vector of vectors’  $\mathbf{b} = (\mathbf{b}_1, \dots, \mathbf{b}_N, \mathbf{b}_T)$  is given by

$$\mathbf{b}_i = \begin{pmatrix} -\sum_{j \neq i} \nabla_{\mathbf{r}_i} \tilde{u}_{ij} + \mathbf{v}^i \\ 0 \end{pmatrix}. \quad (4.17)$$

The third component of this vector equals zero since the angles of the active particles diffuse freely, without a drift. This component is absent when  $i = T$ . Each component of this vector is bounded. Moreover, the diffusion matrix is constant; hence there exists  $C > 0$  such that for all  $\mathbf{x} \in \mathbb{R}^{3N+2}$ ,

$$|\mathbf{b}(\mathbf{x})| + |\sigma(\mathbf{x})| \leq C(1 + |\mathbf{x}|). \quad (4.18)$$

Using Lemmas 4.1 and 4.2, it is straightforwardly shown that each component  $\mathbf{b}_i$  is Lipschitz, and hence  $\mathbf{b}$  itself is Lipschitz. Hence there exists  $c > 0$  such that for all  $\mathbf{x}, \mathbf{y} \in \mathbb{R}^{3N+2}$ ,

$$|\mathbf{b}(\mathbf{x}) - \mathbf{b}(\mathbf{y})| < c|\mathbf{x} - \mathbf{y}|. \quad (4.19)$$

Since the initial positions and angles are given, they are independent of the sigma-algebra generated by  $\mathbf{B}_s$ ,  $s > 0$ . Hence the conditions of Theorem 2.8 are satisfied. □

**Theorem 4.4.** *The probability density  $P$  satisfies the PDE*

$$\partial_t P = - \sum_{i=1}^{N+1} \nabla_{\mathbf{r}_i} \cdot \left( \left( - \sum_{j \neq i} \nabla_{\mathbf{r}_i} \tilde{u}_{ij} + \mathbf{v}^i \right) P \right) + \sum_{i=1}^{N+1} (\sigma^2 \Delta_{\mathbf{r}_i} P + \nu^2 \partial_{\phi_i}^2 P), \quad (4.20)$$

where  $\Delta_{\mathbf{r}_i}$  denotes the Laplace operator with respect to the position variable  $\mathbf{r}_i$ .

*Proof.* The proof that the drift and diffusion coefficients are Lipschitz continuous is analogous to the proof of Theorem 4.3. Hence the stochastic process is indeed an Itô diffusion, and Theorem 2.10 applies.  $\square$

We will always assume that  $\delta \ll 2^{1/6} \sigma_{AA}$ , so that the physics of the system is unchanged, since at the densities we consider the distance between two particles is very unlikely to be smaller than  $\delta$ . We will therefore omit the tilde on the potential and simply write  $u_{ij}$ .

This density defines a probability measure  $\mathbb{P}$ :

$$\mathbb{P}(d\theta_1, \dots, d\theta_N, d\mathbf{z}) = P(\theta_1, \dots, \theta_N, \mathbf{z}) d\theta_1 \cdots d\theta_N d\mathbf{z}, \quad (4.21)$$

where  $d\theta_i := d\mathbf{r}_i d\phi_i = dx_i dy_i d\phi_i$ . Then, by the disintegration theorem [22] we can write  $\mathbb{P}$  as the product of the marginal probability measure  $p$  of the tracer and a measure  $\hat{\mathbb{P}}$  that depends on the tracer's position  $\mathbf{z}$ :

$$\mathbb{P}(d\theta_1, \dots, d\theta_N, d\mathbf{z}) = p(d\mathbf{z}) \hat{\mathbb{P}}(\mathbf{z}, d\theta_1, \dots, d\theta_N). \quad (4.22)$$

The measure  $\hat{\mathbb{P}}$  can be seen as the conditional probability of the positions of the host particles knowing the position of the tracer. Integrating (4.20) over  $\Lambda^N := (\Omega \times \mathbb{R})^N$  yields a PDE for the tracer's marginal density  $p$ :

$$\partial_t p(\mathbf{z}, t) = \sigma^2 \Delta p(\mathbf{z}, t) + \nabla \cdot \int_{\Lambda^N} \sum_{j=1}^N \nabla u_{Tj}(\mathbf{r}_j - \mathbf{z}) P d\theta_1 \cdots d\theta_N, \quad (4.23)$$

$$= \sigma^2 \Delta p(\mathbf{z}, t) + \nabla \cdot p \int_{\Lambda^N} \sum_{j=1}^N \nabla u_{Tj}(\mathbf{r}_j - \mathbf{z}) \hat{\mathbb{P}}(\mathbf{z}, d\theta_1, \dots, d\theta_N), \quad (4.24)$$

where the gradient denotes differentiation with respect to the position  $\mathbf{z}$  of the tracer.

**Theorem 4.5.** *The integral*

$$\int_{\Lambda^N} \sum_{j=1}^N \nabla u_{Tj}(\mathbf{r}_j - \mathbf{z}) \hat{\mathbb{P}}(\mathbf{z}, d\theta_1, \dots, d\theta_N) \quad (4.25)$$

that appears in (4.24) is independent of the tracer's position  $\mathbf{z}$ .

*Proof.* We define the measure

$$\hat{\mathbb{A}}(\mathbf{z}, d\theta) = \hat{\mathbb{P}}(\mathbf{z}, d\theta, \Omega^{N-1}), \quad (4.26)$$

which is the marginal of a single host particle when the tracer's position is known. We interchange summation and integration, and use indistinguishability of the host particles:

$$\int_{\Lambda^N} \sum_{j=1}^N \nabla u_{Tj}(\mathbf{r}_j - \mathbf{z}) \hat{\mathbb{P}}(\mathbf{z}, d\theta_1, \dots, d\theta_N) = N \nabla \cdot p \int_{\Lambda} \nabla u_T(\mathbf{r} - \mathbf{z}) \hat{\mathbb{A}}(\mathbf{z}, d\mathbf{r}, d\phi), \quad (4.27)$$

where we have written  $u_T = u_{Tj}$  for all  $j = 1, \dots, N$ . We henceforth omit the subscript  $j$  since all  $u_{Tj}$ s are equal. Now we define the function  $D_{\mathbf{z}} : \Lambda \rightarrow \Lambda - \mathbf{z} : (\mathbf{r}, \phi) \mapsto (\mathbf{r} - \mathbf{z}, \phi) =: (\mathbf{y}, \phi)$ , where  $\Lambda - \mathbf{z} := \{\mathbf{r} - \mathbf{z} : \mathbf{r} \in \Omega\} \times \mathbb{R}$ .

Then it follows that

$$\nabla u_T(\mathbf{r} - \mathbf{z}) = -(\nabla u_T \circ D_{\mathbf{z}})(\mathbf{r}), \quad (4.28)$$

where we may extend  $u_T$  to be a function on  $\mathbb{R}^3$  that is independent of its third argument. Hence

$$N \nabla \cdot p \int_{\Lambda} \nabla u_T(\mathbf{r} - \mathbf{z}) \hat{\mathbb{A}}(\mathbf{z}, d\mathbf{r}, d\phi) = -N \nabla \cdot p \int_{\Lambda} (\nabla u_T \circ D_{\mathbf{z}})(\mathbf{r}) \hat{\mathbb{A}}(\mathbf{z}, d\theta), \quad (4.29)$$

$$= -N \nabla \cdot p \int_{\Lambda - \mathbf{z}} \nabla u_T(\mathbf{r}) (D_{\mathbf{z}\#} \hat{\mathbb{A}})(\mathbf{z}, d\theta), \quad (4.30)$$

by the change of variables formula, where  $(D_{\mathbf{z}\#} \hat{\mathbb{A}})(\mathbf{z}, d\theta)$  is the push-forward of  $\hat{\mathbb{A}}$  under  $D_{\mathbf{z}}$ :

$$(D_{\mathbf{z}\#} \hat{\mathbb{A}})(\mathbf{z}, O) := \hat{\mathbb{A}}(\mathbf{z}, D_{\mathbf{z}}^{-1}(O)), \quad (4.31)$$

for  $O \subset \Lambda - \mathbf{z}$ .

Suppose the position  $\mathbf{z}$  of the tracer is known and fixed. Set  $\mathbf{Y}_t^i = \mathbf{R}_t^i - \mathbf{z}$ . Then we have that, for  $O \subset \Lambda - \mathbf{z}$  measurable,

$$\text{“Probability for } (\mathbf{Y}_t^i, \Phi_t^i) \in O \text{”} = \text{“Probability for } (\mathbf{R}_t^i, \Phi_t^i) \in O + \mathbf{z} \text{”}, \quad (4.32)$$

where

$$O + \mathbf{z} := \{(\mathbf{r} + \mathbf{z}, \phi) : (\mathbf{r}, \phi) \in O\} \subset \Lambda. \quad (4.33)$$

Hence, if we define  $\hat{\mathbb{F}} := \text{Law}(\mathbf{Y}_t^i, \Phi_t^i)$ , then

$$\hat{\mathbb{F}}(O) = \hat{\mathbb{A}}(\mathbf{z}, O + \mathbf{z}) = (D_{\mathbf{z}\#} \hat{\mathbb{A}})(\mathbf{z}, O). \quad (4.34)$$

Moreover, we have the following SDEs for  $\mathbf{Y}_t^i$ .

$$d\mathbf{Y}_t^i = \left( - \sum_{j \neq i} \nabla_{\mathbf{r}_i} u_{ij}(\mathbf{Y}_t^i - \mathbf{Y}_t^j) - \nabla_{\mathbf{r}_i} u_{Ti}(\mathbf{Y}_t^i) + \mathbf{v}^i(\Phi_t^i) \right) dt + \sqrt{2}\sigma d\mathbf{B}_t^i, \quad (4.35a)$$

$$d\Phi_t^i = \sqrt{2\nu} dB_{\phi,t}^i. \quad (4.35b)$$

Note that these SDEs are independent of the tracer's position  $\mathbf{z}$ . Hence, we also have that  $\hat{\mathbb{F}}$  is independent of  $\mathbf{z}$ , so that the entire quantity

$$\nabla u_T(\mathbf{r}) (D_{\mathbf{z}\#} \hat{\mathbb{A}})(\mathbf{z}, d\theta) \quad (4.36)$$

is constant in  $\mathbf{z}$ . Moreover, due to the periodic boundary conditions,  $\Lambda$  and  $\Lambda - \mathbf{z}$  constitute the same set. Hence the entire integral

$$\int_{\Lambda - \mathbf{z}} \nabla u_T(\mathbf{r}) (D_{\mathbf{z}\#} \hat{\mathbb{A}})(\mathbf{z}, d\theta) \quad (4.37)$$

is independent of  $\mathbf{z}$ .  $\square$

We define

$$(D_{\mathbf{z}\#\hat{\mathbb{A}}})(\mathbf{z}, d\theta) := f(\theta) d\theta, \quad (4.38)$$

so that  $f$  is the one-particle marginal density function for  $\{\mathbf{Y}_t^i, \Phi_t^i\}$ . Since  $(D_{\mathbf{z}\#\hat{\mathbb{A}}})(\mathbf{z}, d\theta)$  is independent of the value of  $\mathbf{z}$ , we can set  $\mathbf{z} = 0$  without loss of generality. Hence  $p$  satisfies

$$\partial_t p = \sigma^2 \Delta p - N \nabla \cdot \left( p \int_{\Lambda} \nabla u_{\text{T}}(\mathbf{r}) f(\mathbf{r}, \phi) d\theta \right), \quad (4.39)$$

Now we turn our attention to finding an expression for this  $f$ , the probability density of  $\hat{\mathbb{A}}$ .

## 4.2 Probability density of a host particle

**Theorem 4.6.** *The Fokker-Planck equation for the probability density  $A$  corresponding to the SDE (4.35) is*

$$\partial_t A = \sum_{i=1}^N \nabla_{\mathbf{r}_i} \cdot (A \nabla_{\mathbf{r}_i} U^i - \mathbf{v}^i A + \sigma^2 \nabla_{\mathbf{r}_i} A) + \sum_{i=1}^N \nu^2 \partial_{\phi_i}^2 A, \quad (4.40)$$

where

$$U^i = \sum_{j \neq i} u_{ij}(\mathbf{r}_i - \mathbf{r}_j) + u^{\text{T}i}(\mathbf{r}_i). \quad (4.41)$$

*Proof.* The proof is analogous to the proof of Theorem 4.4.  $\square$

Next, we integrate  $A$  over  $\Lambda^{N-1}$ , so that we find the marginal  $f$  of a single host particle. The conditions on  $A$  and its derivatives are necessary so as to be able to interchange integration and differentiation.

**Theorem 4.7.** *Suppose  $\partial_t A(t, \theta_1, \dots, \theta_N)$  and  $\partial_{\phi_1} A(t, \mathbf{r}_1, \phi_1, \theta_2, \dots, \theta_N)$  exist for all  $t > 0$ ,  $\mathbf{r}_1 \in \Omega$ ,  $\phi_1 \in \mathbb{R}$ , and for almost all  $(\theta_2, \dots, \theta_N) \in \Lambda^{N-1}$ . Moreover, suppose there exist integrable  $M_t : \Lambda^N \rightarrow \mathbb{R}$  and  $M_{\phi_1} : \mathbb{R}_+ \times \Omega \times \Lambda^{N-1} \rightarrow \mathbb{R}$  such that  $|\partial_t A(t, \theta_1, \dots, \theta_N)| \leq M_t(\theta_1, \dots, \theta_N)$  for all  $t > 0$ ,  $\theta_1 \in \Lambda$  and almost all  $(\theta_2, \dots, \theta_N) \in \Lambda^{N-1}$ , and  $|\partial_{\phi_1} A(t, \mathbf{r}_1, \phi_1, \theta_2, \dots, \theta_N)| \leq M_{\phi_1}(t, \mathbf{r}_1, \theta_2, \dots, \theta_N)$  for all  $t > 0$ ,  $\theta_1 \in \Lambda$  and almost all  $(\theta_2, \dots, \theta_N) \in \Lambda^{N-1}$ . Furthermore, suppose  $\partial_{\phi_i} A \rightarrow 0$  as  $\phi_i \rightarrow \pm\infty$  for all  $i = 1, \dots, N$ . Then the marginal  $f$  of a single host particle satisfies the PDE*

$$\partial_t f = \nabla \cdot [f \nabla u_{\text{T}}(\mathbf{r}_1) - \mathbf{v} f + \sigma^2 \nabla f] + \nu^2 \partial_{\phi}^2 f + \nabla \cdot \int_{\Lambda^{N-1}} A \nabla u^1 d\theta_2 \cdots d\theta_N, \quad (4.42)$$

where the gradient denotes differentiation with respect to the particle's position  $\mathbf{r}_1$  and  $u^1$  is the interaction potential of the first host particle with all other host particles.

The assumptions on  $A$  are reasonable, since the angle  $\phi_1$  can diffuse freely on  $\mathbb{R}$ . We will henceforth assume that these assumptions hold.

*Proof.* We integrate (4.40) over  $\Lambda^{N-1}$  and use Leibniz's rule to interchange differentiation and integration:

$$\begin{aligned} \partial_t f &= \int_{\Lambda^{N-1}} \sum_{i=1}^N \nabla_{\mathbf{r}_i} \cdot (A \nabla_{\mathbf{r}_i} U^i - \mathbf{v}^i A + \sigma^2 \nabla_{\mathbf{r}_i} A) d\theta_2 \cdots d\theta_N \\ &\quad + \int_{\Lambda^{N-1}} \sum_{i=1}^N \nu^2 \partial_{\phi_i}^2 A d\theta_2 \cdots d\theta_N. \end{aligned} \quad (4.43)$$

To the first integral, we apply the divergence theorem and use the periodic boundary conditions. This implies that for  $i = 2, \dots, N$  each term

$$\int_{\Lambda^{N-1}} \nabla_{\mathbf{r}_i} \cdot (A \nabla_{\mathbf{r}_i} U^i - \mathbf{v}^i A + \sigma^2 \nabla_{\mathbf{r}_i} A) d\theta_2 \cdots d\theta_N \quad (4.44)$$

vanishes, and

$$\begin{aligned} &\int_{\Lambda^{N-1}} \sum_{i=1}^N \nabla_{\mathbf{r}_i} \cdot (A \nabla_{\mathbf{r}_i} U^i - \mathbf{v}^i A + \sigma^2 \nabla_{\mathbf{r}_i} A) d\theta_2 \cdots d\theta_N \\ &= \nabla_{\mathbf{r}_1} \cdot [f \nabla_{\mathbf{r}_1} u_T(\mathbf{r}_1) - \mathbf{v}^1 f + \sigma^2 \nabla_{\mathbf{r}_1} f] + \nabla_{\mathbf{r}_1} \cdot \int_{\Lambda^{N-1}} A \nabla_{\mathbf{r}_1} u^1 d\theta_2 \cdots d\theta_N. \end{aligned} \quad (4.45)$$

Since  $\partial_{\phi_i} A \rightarrow 0$  as  $\phi_i \rightarrow \pm\infty$  for all  $i = 1, \dots, N$ , the second integral becomes

$$\int_{\Lambda^{N-1}} \sum_{i=1}^N \nu^2 \partial_{\phi_i}^2 A d\theta_2 \cdots d\theta_N = \nu^2 \int_{\Lambda^{N-1}} \partial_{\phi_1}^2 A d\theta_2 \cdots d\theta_N = \nu^2 \partial_{\phi_1}^2 f \quad (4.46)$$

after interchange of integration and differentiation, again upon application of Leibniz's rule.  $\square$

Our goal in this section is to find an approximate solution for (4.42). We make the following approximations:

1. The host particles are independent. This means that we set the integral term in (4.42) to zero.
2. We look at the long-time limit, so that the distribution of the hosts has equilibrated and  $\partial_t f = 0$ .
3. The initial angle is given by  $\phi_0 \in [0, 2\pi]$ . Then the expectation value of  $\mathbf{v}(\phi)$  is given by (Lemma 2.12)

$$\mathbb{E}[\mathbf{v}] = \exp\left(-\frac{t\nu^2}{2}\right) (\cos(\nu\phi_0), \sin(\nu\phi_0)). \quad (4.47)$$

Moreover, we take  $t = 1/\nu^2$ , the characteristic time scale for rotational diffusion [1], and write

$$\bar{\mathbf{v}} := \frac{\nu_0}{\sqrt{e}} (\cos(\nu\phi_0), \sin(\nu\phi_0)) \quad (4.48)$$

We replace  $\mathbf{v}$  by this constant quantity.

4. We neglect the term  $\nu^2 \partial_{\phi_1}^2 f$ , which accounts for the diffusion of the host particle's angle. Hence  $f$  is constant in  $\phi_1$ .

Then the Fokker-Planck equation reduces to

$$\nabla \cdot [f \nabla u_T - \bar{\mathbf{v}} f + \sigma^2 \nabla f] = 0, \quad (4.49)$$

on  $\Lambda$ , with periodic boundary conditions, and in distributional sense. Since we only consider one host particle, we write  $\mathbf{r}_1 = \mathbf{r}$  and  $\phi_1 = \phi$ .

Outside the disk  $B(r_c, 0)$ , we approximate  $f$  as constant; we set  $f = C \delta(\phi - \phi_0)$  here. This is a reasonable approximation, since the system is assumed to be in steady state. Inside  $B(r_c, 0)$ , we take

$$f(\mathbf{r}, \phi) = C \exp\left(\frac{\bar{\mathbf{v}} \cdot \mathbf{r} - u_T(\mathbf{r})}{\sigma^2}\right) \delta(\phi - \phi_0), \quad (4.50)$$

as this is a solution to (4.49) on the interior of  $B(r_c, 0)$  (in distributional sense). Taking these solutions together, we have

$$f(\mathbf{r}, \phi) = \begin{cases} C \exp\left(\frac{\bar{\mathbf{v}} \cdot \mathbf{r} - u_T(\mathbf{r})}{\sigma^2}\right) \delta(\phi - \phi_0) & \text{if } \mathbf{r} \in B(r_c, 0), \\ C \delta(\phi - \phi_0) & \text{if } \mathbf{r} \notin B(r_c, 0). \end{cases} \quad (4.51)$$

The exact value of  $f$  outside  $B(r_c, 0)$  is actually of minor interest to us; since the potential  $u_T$  is zero on  $\Omega \setminus B(r_c, 0)$ , also the product  $f \nabla u_T = 0$  on  $\Omega \setminus B(r_c, 0)$ . Hence the value of  $f$  outside  $B(r_c, 0)$  only appears as a normalisation constant  $C$  in the integral in (4.39).

The normalisation constant  $C$  is given by

$$\frac{1}{C} = \int_{B(r_c, 0)} \exp\left(\frac{\bar{\mathbf{v}} \cdot \mathbf{r} - u_T(\mathbf{r})}{\sigma^2}\right) d\mathbf{r} + \mathcal{L}(\Omega), \quad (4.52)$$

where  $\mathcal{L}(\Omega)$  is the Lebesgue measure of  $\Omega$ . If  $\Omega \gg B(r_c, 0)$ , we have  $C \approx 1/\mathcal{L}(\Omega)$ . We will use this result when we apply the thermodynamic limit in the following section.

### 4.3 MSD estimation

If we substitute the solution (4.51) to the simplified Fokker-Planck equation (4.49) in the Fokker-Planck equation for the tracer (4.39), we find

$$\begin{aligned} \partial_t p &= \sigma^2 \Delta p \\ &- N \nabla \cdot \left( p C \int_{\Lambda} \nabla u_T(\mathbf{r}) \exp\left(\frac{\bar{\mathbf{v}} \cdot \mathbf{r} - u_T(\mathbf{r})}{\sigma^2}\right) \delta(\phi - \phi_0) d\theta \right), \end{aligned} \quad (4.53)$$

Now we apply the thermodynamic limit, so that  $C \approx 1/\mathcal{L}(\Omega)$  and  $NC \rightarrow \rho$ , the particle number density. Moreover, we define the vector

$$\Xi := - \int_{\Omega} (\nabla u_T(\mathbf{r})) \exp\left(\frac{\bar{\mathbf{v}} \cdot \mathbf{r} - u_T(\mathbf{r})}{\sigma^2}\right) d\mathbf{r}, \quad (4.54)$$

which is constant in  $t$  and  $\mathbf{z}$ . Hence (4.53) becomes

$$\partial_t p = \sigma^2 \Delta p + \rho \Xi \cdot \nabla p \quad (4.55a)$$

$$p(0, \mathbf{z}) = \delta(\mathbf{z}). \quad (4.55b)$$

**Lemma 4.8.** *The PDE (4.55) on  $\mathbb{R}_+ \times \mathbb{R}^2$  is solved by*

$$p(t, \mathbf{z}) = \frac{1}{4\pi\sigma^2 t} \exp\left(-\frac{|\mathbf{z} + \rho t \Xi|^2}{4\sigma^2 t}\right). \quad (4.56)$$

*in space-distributional sense.*

*Proof.* Let  $\psi : \mathbb{R}^2 \rightarrow \mathbb{R}$  be a test function. We treat  $t$  as a parameter, so we have to show that

$$\frac{d}{dt} \int_{\mathbb{R}^2} p(t, \mathbf{z}) \psi(\mathbf{z}) d\mathbf{z} = \sigma^2 \int_{\mathbb{R}^2} p(t, \mathbf{z}) ((\Delta \psi)(\mathbf{z})) d\mathbf{z} + \rho \Xi \cdot \int_{\mathbb{R}^2} p(t, \mathbf{z}) \nabla \psi(\mathbf{z}) d\mathbf{z}. \quad (4.57)$$

for all  $t > 0$ , with  $p(t, \mathbf{z})$  given by (4.56). This equality can easily be verified by partial integration and noting that  $\psi(\mathbf{z})$  and all its derivatives approach 0 as  $|\mathbf{z}| \rightarrow \infty$ . Moreover, we show that

$$\lim_{t \rightarrow 0} \int_{\mathbb{R}^2} \frac{1}{4\pi\sigma^2 t} \exp\left(-\frac{|\mathbf{z} + \rho t \Xi|^2}{4\sigma^2 t}\right) \psi(\mathbf{z}) d\mathbf{z} = \psi(0) = \delta(\psi). \quad (4.58)$$

To this extent, let  $\varepsilon > 0$ . Choose  $\delta > 0$  such that  $|\psi(\mathbf{z}) - \psi(0)| < \varepsilon$  for all  $|\mathbf{z}| < \delta$ . Let  $t > 0$  such that  $B(-\rho t \Xi, \delta/2) \subset B(0, \delta)$ . Then

$$\left| \int_{\mathbb{R}^2} p(t, \mathbf{z}) \psi(\mathbf{z}) d\mathbf{z} - \psi(0) \right| = \left| \int_{\mathbb{R}^2} p(t, \mathbf{z}) (\psi(\mathbf{z}) - \psi(0)) d\mathbf{z} \right| \quad (4.59)$$

$$\leq \int_{B(-\rho t \Xi, \delta/2)} p(t, \mathbf{z}) |\psi(\mathbf{z}) - \psi(0)| d\mathbf{z} + \int_{\mathbb{R}^2 \setminus B(-\rho t \Xi, \delta/2)} p(t, \mathbf{z}) |\psi(\mathbf{z}) - \psi(0)| d\mathbf{z}, \quad (4.60)$$

The first integral after the inequality can be estimated by

$$\int_{B(-\rho t \Xi, \delta/2)} p(t, \mathbf{z}) |\psi(\mathbf{z}) - \psi(0)| d\mathbf{z} \leq \varepsilon \int_{\mathbb{R}^2} p(t, \mathbf{z}) d\mathbf{z} = \varepsilon. \quad (4.61)$$

For the second integral, we know that there exists  $M \geq 0$  such that for all  $\mathbf{y} \in \mathbb{R}^2$ ,  $|\psi(\mathbf{y}) - \psi(0)| \leq M$ . Hence

$$\begin{aligned} & \int_{\mathbb{R}^2 \setminus B(-\rho t \Xi, \delta/2)} p(t, \mathbf{z}) |\psi(\mathbf{z}) - \psi(0)| d\mathbf{z} \\ & \leq \frac{M}{4\pi\sigma^2 t} \int_{\mathbb{R}^2 \setminus B(-\rho t \Xi, \delta/2)} \exp\left(-\frac{|\mathbf{z} + \rho t \Xi|^2}{4\sigma^2 t}\right) d\mathbf{y}. \end{aligned} \quad (4.62)$$

Then, by a change of variables  $\mathbf{y} = \mathbf{z} + \rho t \Xi$ ,

$$\int_{\mathbb{R}^2 \setminus B(-\rho t \Xi, \delta/2)} p(t, \mathbf{z}) |\psi(\mathbf{z}) - \psi(0)| d\mathbf{z} \leq \frac{M}{4\pi\sigma^2 t} \int_{B(0, \delta/2)} \exp\left(-\frac{|\mathbf{y}|^2}{4\sigma^2 t}\right) d\mathbf{y} \quad (4.63)$$

$$= \frac{M}{2\sigma^2 t} \int_{\delta/2}^{\infty} \exp\left(-\frac{r^2}{4\sigma^2 t}\right) r dr \rightarrow 0 \text{ as } t \downarrow 0. \quad (4.64)$$



Hence, for  $t > 0$  sufficiently small,

$$\left| \int_{\mathbb{R}^2} p(t, \mathbf{z}) \psi(\mathbf{z}) \, d\mathbf{z} - \psi(0) \right| < 2\varepsilon. \quad (4.65)$$

□

**Lemma 4.9.** *The quantity  $|\Xi|^2$  is independent of  $\phi_0$ .*

*Proof.* We show that the derivative of  $|\Xi|^2$  with respect to  $\phi_0$  equals 0. We have

$$\frac{d|\Xi|^2}{d\phi_0} = 2\Xi \cdot \frac{d\Xi}{d\phi_0}. \quad (4.66)$$

To evaluate this expression, we convert the integrals to polar coordinates  $(s, \alpha)$ . Then the  $x$ -component of  $\Xi$  reads

$$\begin{aligned} \Xi_x = & - \int_0^{r_c} \int_0^{2\pi} \left( -12 \left( \frac{\sigma_{AT}}{s} \right)^{12} + 6 \left( \frac{\sigma_{AT}}{s} \right)^6 \right) \cos(\alpha) \\ & \exp \left( \frac{v_0 e^{-1/2} s \cos(\nu\phi_0 - \alpha) - u_T(s)}{\sigma^2} \right) s \, d\alpha \, ds, \end{aligned} \quad (4.67)$$

where we write  $u_T(s) = u_T(x, y)$  with  $\sqrt{x^2 + y^2} = s$  by abuse of notation. The integral over  $\alpha$  equals

$$\begin{aligned} & \int_0^{2\pi} \cos(\alpha) \exp(\beta \cos(\nu\phi_0 - \alpha)) \, d\alpha \\ &= \cos(\nu\phi_0) \int_0^{2\pi} \cos(\eta) \exp(\beta \cos(\eta)) \, d\eta - \sin(\nu\phi_0) \int_0^{2\pi} \sin(\eta) \exp(\beta \cos(\eta)) \, d\eta \end{aligned} \quad (4.68)$$

where we write  $\beta := v_0 e^{-1/2} s / \sigma^2$ . The second integral after the equality sign equals 0 since the integrand is an odd function about  $\pi$ , but the first integral equals

$$\cos(\nu\phi_0) \int_0^{2\pi} \cos(\eta) \exp(\beta \cos(\eta)) \, d\eta = 2\pi \cos(\nu\phi_0) I_1(\beta), \quad (4.69)$$

where  $I_\nu$  is the modified Bessel function of the first kind [23]. Hence

$$\Xi_x = -2\pi \cos(\nu\phi_0) \int_0^{r_c} \left( -12 \left( \frac{\sigma_{AT}}{s} \right)^{12} + 6 \left( \frac{\sigma_{AT}}{s} \right)^6 \right) \exp \left( -\frac{u_T(s)}{\sigma^2} \right) I_1(\beta) \, ds. \quad (4.70)$$

Similarly,

$$\Xi_y = -2\pi \sin(\nu\phi_0) \int_0^{r_c} \left( -12 \left( \frac{\sigma_{AT}}{s} \right)^{12} + 6 \left( \frac{\sigma_{AT}}{s} \right)^6 \right) \exp \left( -\frac{u_T(s)}{\sigma^2} \right) I_1(\beta) \, ds. \quad (4.71)$$

Hence we have

$$\frac{d\Xi_x}{d\phi_0} = -\nu \Xi_y \quad \text{and} \quad \frac{d\Xi_y}{d\phi_0} = \nu \Xi_x, \quad (4.72)$$

which together with (4.66) implies the desired result. □

With this expression, we can find the tracer's MSD as a function of time, which follows by direct integration.

**Theorem 4.10.** *The second moment of the distribution specified by (4.56) is*

$$\text{MSD}(t) = \mathbb{E} \left[ |\mathbf{Z}_t|^2 \right] = 4\sigma^2 t + \rho^2 |\boldsymbol{\Xi}|^2 t^2. \quad (4.73)$$

*Proof.* Let  $t > 0$ . By change of variables  $\mathbf{y} = \mathbf{z} + \rho t \boldsymbol{\Xi}$ , we have

$$\begin{aligned} \mathbb{E} \left[ |\mathbf{Z}_t|^2 \right] &= \int_{\mathbb{R}^2} |\mathbf{z}|^2 p(t, \mathbf{z}) \, d\mathbf{z} \quad (4.74) \\ &= \underbrace{\int_{\mathbb{R}^2} \frac{|\mathbf{y}|^2}{4\pi\sigma^2 t} \exp\left(-\frac{|\mathbf{y}|^2}{4\sigma^2 t}\right) \, d\mathbf{y}}_{=: \text{I}} - \underbrace{\frac{2\rho t \boldsymbol{\Xi}}{4\pi\sigma^2 t} \cdot \int_{\mathbb{R}^2} \mathbf{y} \exp\left(-\frac{|\mathbf{y}|^2}{4\sigma^2 t}\right) \, d\mathbf{y}}_{=: \text{II}} \\ &\quad + \underbrace{\rho^2 t^2 |\boldsymbol{\Xi}|^2 \int_{\mathbb{R}^2} \frac{1}{4\pi\sigma^2 t} \exp\left(-\frac{|\mathbf{y}|^2}{4\sigma^2 t}\right) \, d\mathbf{y}}_{=: \text{III}}. \end{aligned} \quad (4.75)$$

Then, by converting these integrals to polar coordinates  $(r, \alpha)$ ,

$$\text{I} = \frac{1}{4\pi\sigma^2 t} \int_0^{2\pi} \int_0^\infty r^3 \exp\left(-\frac{r^2}{4\sigma^2 t}\right) \, dr \, d\alpha \quad (4.76)$$

$$= 4\sigma^2 t \quad (4.77)$$

by successive application of partial integration. For the second integral,

$$\text{II} = -2\rho t \boldsymbol{\Xi} \cdot \int_0^{2\pi} \int_0^\infty r^2 (\cos(\alpha), \sin(\alpha)) \exp\left(-\frac{r^2}{4\sigma^2 t}\right) \, dr \, d\alpha = 0 \quad (4.78)$$

since the integrals of  $\cos(\alpha)$  and  $\sin(\alpha)$  over a full cycle equal 0. The third integral

$$\text{III} = \frac{\rho^2 t^2 |\boldsymbol{\Xi}|^2}{4\pi\sigma^2 t} \int_0^{2\pi} \int_0^\infty r \exp\left(-\frac{r^2}{4\sigma^2 t}\right) \, dr \, d\alpha = \rho^2 t^2 |\boldsymbol{\Xi}|^2, \quad (4.79)$$

again by partial integration.  $\square$

We can rewrite  $|\boldsymbol{\Xi}|^2$  as follows

$$|\boldsymbol{\Xi}|^2 = 4\pi^2 \sigma^4 \left[ r_c I_1 \left( \frac{v_0}{\sigma^2} \frac{r_c}{\sqrt{e}} \right) - \int_0^{r_c} \exp\left(-\frac{u_{\text{T}}(s)}{\sigma^2}\right) \partial_s \left( s I_1 \left( \frac{v_0}{\sigma^2} \frac{s}{\sqrt{e}} \right) \right) \, ds \right]^2. \quad (4.80)$$

In Figure 4.1,  $|\boldsymbol{\Xi}|^2$  is plotted against  $v_0$  for different values of  $\sigma^2$ . From this plot, it becomes clear that  $|\boldsymbol{\Xi}|^2$  increases with  $v_0$ , whereas it decreases with  $\sigma^2$ .

To summarise, our crude approximations predict the following behaviour for the tracer's MSD:

1. At short times,  $\text{MSD} \approx 4\sigma^2 t$ . At long times,  $\text{MSD} \approx \rho^2 |\boldsymbol{\Xi}|^2 t^2$ . In particular, the tracer's movement is ballistic at long times.

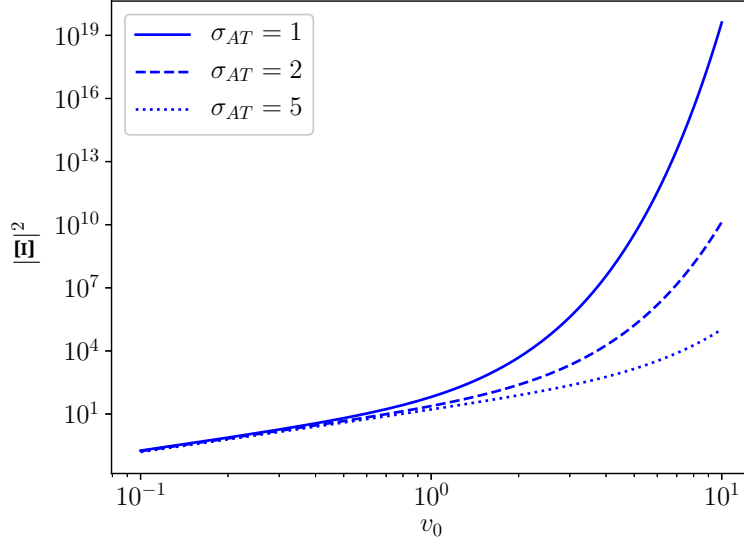


Figure 4.1:  $|\Xi|^2$  for different values of diffusion coefficient  $\sigma^2$  and active velocity  $v_0$ .  $|\Xi|^2$  characterises the strength of the tracer's ballistic diffusion at given density.  $v_0$  ranges from 0 to 25. Clearly,  $|\Xi|^2$  increases as  $v_0$  increases, but decreases as  $\sigma^2$  increases.

2. The MSD increases with particle density  $\rho$ .
3. The MSD increases with active host velocity  $v_0$ .
4. In the ballistic regime, i.e. at large  $t$ , the MSD decreases with diffusion coefficient  $\sigma^2$ . Since  $\sigma^2$  is proportional to the temperature  $T$ , the MSD also decreases with increasing  $T$ .

We present the results of the numerical simulations of the SDEs (3.8) in the following chapter. In Chapter 6 we compare the results of both methods.

#### 4.4 Approximation of host particle density function by matched asymptotic expansions

By using the technique of matched asymptotic expansions, we improve the the approximation for the host particle density (4.51). Again we consider the equation in Theorem 4.6:

$$\partial_t A = \sum_{i=1}^N \nabla_{\mathbf{r}_i} \cdot (A \nabla_{\mathbf{r}_i} U^i - \mathbf{v}^i A + \sigma^2 \nabla_{\mathbf{r}_i} A) + \sum_{i=1}^N \nu^2 \partial_{\phi_i}^2 A. \quad (4.81)$$

Now, we integrate over  $\Lambda^{N-2}$  to find a PDE for the probability density  $P_2$  of the first two particles:

$$\begin{aligned} \partial_t P_2 &= \nabla_{\mathbf{r}_1} \cdot (P_2 \nabla_{\mathbf{r}_1} (u_T(\mathbf{r}_1) + u_{12}(\mathbf{r}_1 - \mathbf{r}_2)) - \mathbf{v}(\phi_1) P_2 + \sigma^2 \nabla_{\mathbf{r}_1} P_2) \\ &\quad + \nabla_{\mathbf{r}_2} \cdot (P_2 \nabla_{\mathbf{r}_2} (u_T(\mathbf{r}_2) + u_{21}(\mathbf{r}_2 - \mathbf{r}_1)) - \mathbf{v}(\phi_2) P_2 + \sigma^2 \nabla_{\mathbf{r}_2} P_2) \\ &+ (N-2) \int_{\Lambda^{N-2}} P_3 \nabla_{\mathbf{r}_1} u_{13}(\mathbf{r}_1 - \mathbf{r}_3) d\theta_3 + (N-2) \int_{\Lambda^{N-2}} P_3 \nabla_{\mathbf{r}_2} u_{23}(\mathbf{r}_2 - \mathbf{r}_3) d\theta_3 \\ &\quad + \nu^2 (\partial_{\phi_1}^2 P_2 + \partial_{\phi_2}^2 P_2). \end{aligned} \quad (4.82)$$

Here,  $P_2 = \int_{\Lambda^{N-2}} A d\theta_3 \cdots d\theta_N$  and  $P_3 = \int_{\Lambda^{N-3}} A d\theta_4 \cdots d\theta_N$  are the two- and three-particle marginal density functions respectively. Again, we make a few simplifications, that are similar to the ones we made before. We take, for  $j = 1, 2$ ,

$$\mathbf{v}(\phi_j) = \bar{\mathbf{v}}(\phi_j) := \frac{v_0}{\sqrt{e}} (\cos(\nu\phi_j), \sin(\nu\phi_j)), \quad (4.83)$$

with  $\phi_j$  fixed. Moreover, we set again the integral terms to 0. This time however, this does not imply that the host particles are independent, but only that they are dilute, so that three-particle interactions are unlikely. Also, we set the angular diffusion terms to 0. Then we have

$$\begin{aligned} \partial_t P_2 &= \nabla_{\mathbf{r}_1} \cdot (P_2 \nabla_{\mathbf{r}_1} (u_T(\mathbf{r}_1) + u_{12}(\mathbf{r}_1 - \mathbf{r}_2)) - \bar{\mathbf{v}}(\phi_1) P_2 + \sigma^2 \nabla_{\mathbf{r}_1} P_2) \\ &\quad + \nabla_{\mathbf{r}_2} \cdot (P_2 \nabla_{\mathbf{r}_2} (u_T(\mathbf{r}_2) + u_{21}(\mathbf{r}_2 - \mathbf{r}_1)) - \bar{\mathbf{v}}(\phi_2) P_2 + \sigma^2 \nabla_{\mathbf{r}_2} P_2). \end{aligned} \quad (4.84)$$

Furthermore, we assume  $P_2$  has the following form:

$$P_2 = Q(\mathbf{r}_1, \mathbf{r}_2) f_1(\mathbf{r}_1) f_2(\mathbf{r}_2), \quad (4.85)$$

with  $Q$  an undetermined function, and for  $j = 1, 2$

$$f_j(\mathbf{r}_j) = C \exp\left(\frac{\bar{\mathbf{v}}(\phi_j) \cdot \mathbf{r}_j - u_T(\mathbf{r}_j)}{\sigma^2}\right), \quad (4.86)$$

i.e. the solution to (4.49). We assume that the particles become independent as their separation goes to infinity, which implies that  $Q \rightarrow C'$  as  $|\mathbf{r}_1 - \mathbf{r}_2| \rightarrow \infty$ , with  $C'$  a normalisation constant. By substituting this ansatz for  $P_2$  into (4.84), we find

$$\begin{aligned} f_1 f_2 \partial_t Q &= \nabla_{\mathbf{r}_1} \cdot (Q f_2 \{f_1 [\nabla_{\mathbf{r}_1} u_T - \bar{\mathbf{v}}(\phi_1)] + \sigma^2 \nabla_{\mathbf{r}_1} f_1\} + \sigma^2 f_1 f_2 \nabla_{\mathbf{r}_1} Q) \\ &\quad + \nabla_{\mathbf{r}_2} \cdot (Q f_1 \{f_2 [\nabla_{\mathbf{r}_2} u_T - \bar{\mathbf{v}}(\phi_2)] + \sigma^2 \nabla_{\mathbf{r}_2} f_2\} + \sigma^2 f_1 f_2 \nabla_{\mathbf{r}_2} Q) \\ &\quad + \nabla_{\mathbf{r}_1} \cdot (f_1 f_2 Q \nabla_{\mathbf{r}_1} u_{12}(\mathbf{r}_1 - \mathbf{r}_2)) + \nabla_{\mathbf{r}_2} \cdot (f_1 f_2 Q \nabla_{\mathbf{r}_2} u_{12}(\mathbf{r}_1 - \mathbf{r}_2)) \end{aligned} \quad (4.87)$$

Since  $f_1$  and  $f_2$  satisfy (4.49), the terms between accolades vanish, and we have

$$\begin{aligned} f_1 f_2 Q &= \nabla_{\mathbf{r}_1} \cdot (\sigma^2 f_1 f_2 \nabla_{\mathbf{r}_1} Q + f_1 f_2 Q \nabla_{\mathbf{r}_1} u_{12}(\mathbf{r}_1 - \mathbf{r}_2)) \\ &\quad + \nabla_{\mathbf{r}_2} \cdot (\sigma^2 f_1 f_2 \nabla_{\mathbf{r}_2} Q + f_1 f_2 Q \nabla_{\mathbf{r}_2} u_{12}(\mathbf{r}_1 - \mathbf{r}_2)) \end{aligned} \quad (4.88)$$

We know that for  $j, k = 1, 2, k \neq j$ ,

$$\nabla_{\mathbf{r}_j} f_j(\mathbf{r}_j) = \frac{1}{\sigma^2} (\bar{\mathbf{v}}(\phi_j) - \nabla_{\mathbf{r}_j} u_T(\mathbf{r}_j)) f_j, \quad \nabla_{\mathbf{r}_k} f_j(\mathbf{r}_j) = 0. \quad (4.89)$$

Hence  $Q$  satisfies, with  $j \neq i$ ,

$$\begin{aligned} \partial_t Q = \sum_{i=1}^2 \left[ \frac{1}{\sigma^2} (\bar{\mathbf{v}}_i - \nabla_{\mathbf{r}_i} u_T(\mathbf{r}_i)) \cdot (\sigma^2 \nabla_{\mathbf{r}_i} Q + Q \nabla_{\mathbf{r}_i} u_{ij}(\mathbf{r}_i - \mathbf{r}_j)) \right. \\ \left. + \nabla_{\mathbf{r}_i} \cdot (\sigma^2 \nabla_{\mathbf{r}_i} Q + Q \nabla_{\mathbf{r}_i} u_{ij}(\mathbf{r}_i - \mathbf{r}_j)) \right] \end{aligned} \quad (4.90)$$

Now, the terms  $\nabla_{\mathbf{r}_i} u_T(\mathbf{r}_i)$ , that represent host-tracer interaction, will cause  $P_2$  to approach 0 as  $\mathbf{r}_i \rightarrow 0$ , for  $i = 1, 2$ . However, since  $P_2 = Q f_1 f_2$  and  $f_i \rightarrow 0$  as  $\mathbf{r}_i \rightarrow 0$ ,  $P_2 \rightarrow 0$  as  $\mathbf{r}_i \rightarrow 0$  regardless of the presence of the terms  $\nabla_{\mathbf{r}_i} u_T(\mathbf{r}_i)$  in (4.90). Hence, we neglect these terms, so that (4.90) simplifies to

$$\begin{aligned} \partial_t Q = \sum_{i=1}^2 \left[ \frac{\bar{\mathbf{v}}_i}{\sigma^2} \cdot (\sigma^2 \nabla_{\mathbf{r}_i} Q + Q \nabla_{\mathbf{r}_i} u_{ij}(\mathbf{r}_i - \mathbf{r}_j)) \right. \\ \left. + \nabla_{\mathbf{r}_i} \cdot (\sigma^2 \nabla_{\mathbf{r}_i} Q + Q \nabla_{\mathbf{r}_i} u_{ij}(\mathbf{r}_i - \mathbf{r}_j)) \right]. \end{aligned} \quad (4.91)$$

We will use the technique of matched asymptotic expansions to find an approximate solution to this equation. We use the fact that the potential is short-ranged, with range  $\epsilon := 2^{1/6} \sigma_{AA} \ll \sqrt{\mathcal{L}(\Omega)}$ , and define two new variables:

$$\tilde{\mathbf{r}}_1 := \mathbf{r}_1 \quad \text{and} \quad \tilde{\mathbf{r}} := \frac{1}{\epsilon} (\mathbf{r}_2 - \mathbf{r}_1). \quad (4.92)$$

Moreover, we define  $\tilde{Q}(\tilde{\mathbf{r}}_1, \tilde{\mathbf{r}}, t) = Q(\mathbf{r}_1, \mathbf{r}_2, t)$  and  $\tilde{u}_{12}(\tilde{\mathbf{r}}) = u_{12}(\mathbf{r}_1 - \mathbf{r}_2)$ . In terms of the variables  $\tilde{\mathbf{r}}_1$  and  $\tilde{\mathbf{r}}$ , the gradient operators become

$$\nabla_{\mathbf{r}_1} = \nabla_{\tilde{\mathbf{r}}_1} - \frac{1}{\epsilon} \nabla_{\tilde{\mathbf{r}}} \quad \text{and} \quad \nabla_{\mathbf{r}_2} = \frac{1}{\epsilon} \nabla_{\tilde{\mathbf{r}}}. \quad (4.93)$$

Rewriting (4.91) in terms of these newly defined functions and variables, and grouping terms of same order in  $\epsilon$ , we find

$$\begin{aligned} \epsilon^2 \partial_t \tilde{Q} = 2 \left[ \sigma^2 \Delta_{\tilde{\mathbf{r}}} \tilde{Q} + \nabla_{\tilde{\mathbf{r}}} \cdot (\tilde{Q} \nabla_{\tilde{\mathbf{r}}} \tilde{u}_{12}(\tilde{\mathbf{r}})) \right] \\ + \epsilon \left[ (\bar{\mathbf{v}}_2 - \bar{\mathbf{v}}_1) \cdot \left( \nabla_{\tilde{\mathbf{r}}} \tilde{Q} + \tilde{Q} \nabla_{\tilde{\mathbf{r}}} \left( \frac{\tilde{u}_{12}(\tilde{\mathbf{r}})}{\sigma^2} \right) \right) - \nabla_{\tilde{\mathbf{r}}_1} \cdot \left( 2\sigma^2 \nabla_{\tilde{\mathbf{r}}} \tilde{Q} + \tilde{Q} \nabla_{\tilde{\mathbf{r}}} \tilde{u}_{12}(\tilde{\mathbf{r}}) \right) \right] \\ + \epsilon^2 \left[ \bar{\mathbf{v}}_1 \cdot \nabla_{\tilde{\mathbf{r}}_1} \tilde{Q} + \sigma^2 \Delta_{\tilde{\mathbf{r}}_1} \tilde{Q} \right]. \end{aligned} \quad (4.94)$$

We seek a solution to this equation of the form

$$\tilde{Q} = \tilde{Q}_0 + \epsilon \tilde{Q}_1 + \dots \quad (4.95)$$

Then the 0th-order problem becomes

$$2 \left( \sigma^2 \Delta_{\tilde{\mathbf{r}}} \tilde{Q}_0 + \nabla_{\tilde{\mathbf{r}}} \cdot (\tilde{Q}_0 \nabla_{\tilde{\mathbf{r}}} \tilde{u}_{12}(\tilde{\mathbf{r}})) \right) = 0 \quad (4.96)$$

with  $\tilde{Q}_0 \rightarrow 1$  as  $\tilde{\mathbf{r}} \rightarrow \infty$ . The solution to this equation is given by

$$\tilde{Q}_0 = \exp \left( -\frac{\tilde{u}_{12}(\tilde{\mathbf{r}})}{\sigma^2} \right). \quad (4.97)$$

The 1st-order problem reads

$$2 \left( \sigma^2 \Delta_{\tilde{\mathbf{r}}} \tilde{Q}_1 + \nabla_{\tilde{\mathbf{r}}} \cdot (\tilde{Q}_1 \nabla_{\tilde{\mathbf{r}}} \tilde{u}_{12}(\tilde{\mathbf{r}})) \right) + (\tilde{\mathbf{v}}_2 - \tilde{\mathbf{v}}_1) \cdot \left( \nabla_{\tilde{\mathbf{r}}} \tilde{Q}_0 + \tilde{Q}_0 \nabla_{\tilde{\mathbf{r}}} \left( \frac{\tilde{u}_{12}(\tilde{\mathbf{r}})}{\sigma^2} \right) \right) - \nabla_{\tilde{\mathbf{r}}_1} \cdot \left( 2\sigma^2 \nabla_{\tilde{\mathbf{r}}} \tilde{Q}_0 + \tilde{Q}_0 \nabla_{\tilde{\mathbf{r}}} \tilde{u}_{12}(\tilde{\mathbf{r}}) \right) = 0. \quad (4.98)$$

All terms involving  $\tilde{Q}_0$  vanish, because of (4.97) and because  $\tilde{Q}_0$  is independent of  $\tilde{\mathbf{r}}_1$ . Hence

$$\tilde{Q}_1 = \exp \left( -\frac{\tilde{u}_{12}(\tilde{\mathbf{r}})}{\sigma^2} \right), \quad (4.99)$$

so that

$$P_2(\mathbf{r}_1, \phi_1, \mathbf{r}_2, \phi_2) = C' \exp \left( -\frac{\tilde{u}_{12}(\tilde{\mathbf{r}})}{\sigma^2} \right) f_1(\mathbf{r}_1) f_2(\mathbf{r}_2), \quad (4.100)$$

with  $C'$  a normalisation constant.

In terms of  $P_2$ , the tracer's probability density satisfies

$$\partial_t p = \sigma^2 \Delta p - N \nabla \cdot \left( p \int_{\Lambda^2} (\nabla_{\mathbf{r}_1} u_T(\mathbf{r}_1)) P_2(\theta_1, \theta_2) d\theta_1 d\theta_2 \right). \quad (4.101)$$

This implies a similar MSD profile for the tracer, only with different constants:

$$\text{MSD}(t) = 4\sigma^2 t + |\Xi'|^2 t^2, \quad (4.102)$$

with

$$\Xi' := -N \int_{\Lambda^2} (\nabla_{\mathbf{r}_1} u_T(\mathbf{r}_1)) P_2(\theta_1, \theta_2) d\theta_1 d\theta_2. \quad (4.103)$$

Further evaluation of the constant  $\Xi'$  can be the topic of future research.

## Chapter 5

# Simulation Results

The subject of this Chapter is the investigation of the tracer's MSD profile as a function of temperature, active velocity and particle density. We do this by numerically solving the system (3.8).

In Figure 5.1 we plot the MSD as a function of time for three different velocities  $v_0$ , but equal temperature and density. This Figure already indicates that the tracer's diffusive behaviour is significantly enhanced due to the activity of the bath particles. We can identify three regimes: For very short times, the MSD grows linearly in time. At intermediate times, the MSD is proportional to  $t^\alpha$  with  $\alpha < 1$  or  $\alpha > 1$  depending on the activity. At  $v_0 = 0$ , we observe that  $\alpha < 1$  and the tracer's diffusion is subdiffusive. As  $v_0$  increases,  $\alpha$  increases to a value larger than 1. At long times, the diffusion becomes normal again, but with a different proportionality factor than the short time diffusion.

Similar behaviour is found at other densities, activities and velocities. In Section 5.1 we briefly look at the short-time characteristics of the MSD. Section 5.2 outlines the intermediate regime and we explore how  $\alpha$  changes with area fraction, temperature and activity. In Section 5.3 the long-time effective diffusion coefficient as a function of the aforementioned three variables is characterised.

### 5.1 Short-time regime

At short times, the tracer's MSD is linear in time. This can be explained by the fact that the tracer has not yet had the opportunity to interact with the bath particles, so that the tracer behaves as a freely diffusing particle whose position satisfies the SDE

$$d\mathbf{Z}_t = \sqrt{2D_0} d\mathbf{B}_t, \quad (5.1)$$

where  $D_0$  is the short-time diffusion constant of the tracer. For such a particle we have  $\text{MSD} = 4D_0t$ , as we saw in Section 2.5. Because of our choice of values for the simulation, the proportionality constant equals  $4D_0 = 4T$ . To extract a value for  $D_0$  from the MSD profile, we define

$$D_0 := \frac{1}{4} \lim_{t \rightarrow 0} \left( \frac{d}{dt} \text{MSD}(t) \right), \quad (5.2)$$

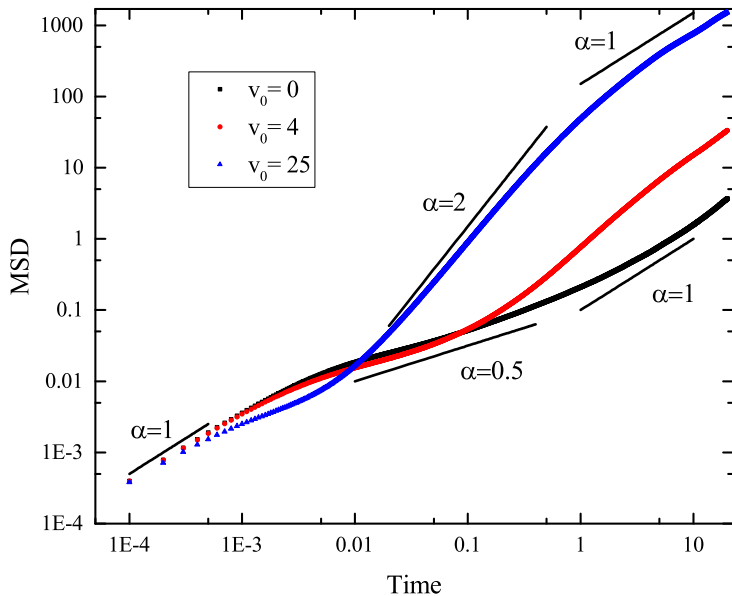


Figure 5.1: MSD of the tracer against time for different velocities  $v_0$  of the hosts. In each case, temperature  $T = 1$  and area fraction  $f = (\pi/4)\rho = 0.628$ , with  $\rho$  the dimensionless density. At very short times,  $\text{MSD} \sim t$ , whereas at intermediate times  $\text{MSD} \sim t^\alpha$ , with  $\alpha < 1$  for low  $v_0$  and  $\alpha > 1$  for high  $v_0$ . At long times,  $\text{MSD} \sim t$  again.

and we determine  $D_0$  from the MSD's slope at short times. The expected behaviour is indeed observed, independent of bath activity and density: we find that  $D_0 = pT + q$ , with  $p = 0.997 \pm 0.0001$  and  $q = 0.002 \pm 0.002$ . The slope  $p$  being just below 1 can be attributed to the fact that the two points in time that we use to measure  $D_0$  are too far apart; decreasing the time step size will cause the measured value of  $D_0$  to become closer to 1. In particular, at high temperature, velocity and/or density the time until the first tracer-host interaction is extremely small.

## 5.2 Intermediate regime

Next, we look at the intermediate regime, in which  $\text{MSD} \sim t^\alpha$  with  $\alpha \neq 1$ . In Figure 5.2 we plot the values for  $\alpha$  against the dimensionless Péclet number  $\text{Pe}$ , which we define as

$$\text{Pe} := \frac{v_0}{\sqrt{D_T D_R}}. \quad (5.3)$$

This number characterises the importance of the activity of the bath particles compared to thermal fluctuations [1]. At low  $\text{Pe}$ , the thermal fluctuations dominate and the tracer behaves as if its environment is passive. On the other hand, at high  $\text{Pe}$  the activity of the hosts dominates and the interactions between the tracer and the fluid molecules are less important. Because of our choice of values for the constants in the numerical simulations we have that  $D_T = D_R = T$ , so



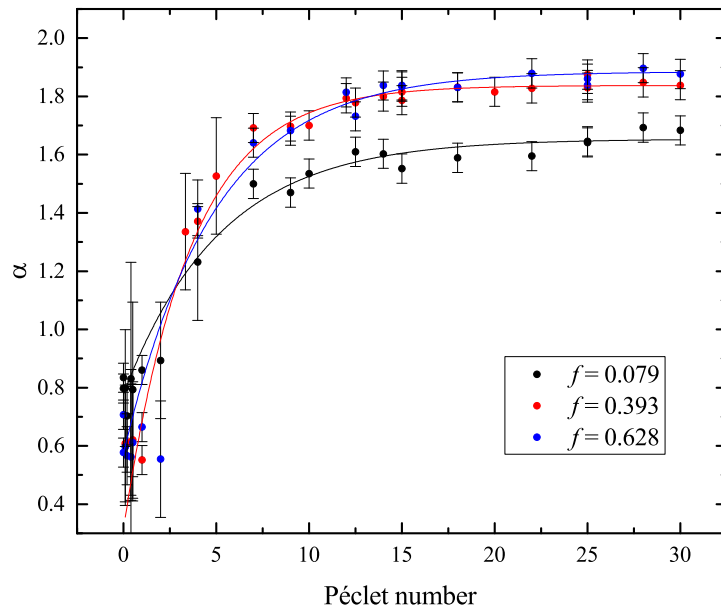


Figure 5.2: Anomalous exponent  $\alpha$  at intermediate times against the Péclet number  $Pe \sim v_0/T$  for different area fractions  $f$ .  $Pe$  characterises the importance of the activity relative to the thermal fluctuations in the supporting fluid. At low  $Pe$ , the thermal fluctuations dominate and  $\alpha < 1$ , implying subdiffusive motion of the tracer. At high  $Pe$ , activity dominates and  $\alpha > 1$ , so that the tracer’s dynamics are superdiffusive. The fits are made using (5.5).

that

$$Pe = \frac{v_0}{T}. \quad (5.4)$$

At low  $Pe$ , we observe  $\alpha < 1$ , which means that the tracer performs a subdiffusive movement. However, at high  $Pe$ ,  $\alpha > 1$  and the motion of the tracer is superdiffusive. Moreover,  $\alpha$  approaches a constant value strictly smaller than 2 as  $Pe \rightarrow \infty$ , so that the motion of the tracer never truly becomes ballistic. Moreover, this limiting value seems to depend on the bath density. We introduce the following ad hoc ansatz for  $\alpha$  as a function of  $Pe$ :

$$\alpha = \alpha_0 \left( 1 - c \exp\left(-\frac{Pe}{Pe_0}\right) \right), \quad (5.5)$$

where  $\alpha_0$ ,  $c$  and  $Pe_0$  are fit parameters. In particular,  $\alpha \rightarrow \alpha_0$  as  $Pe \rightarrow \infty$ . Table 5.1 depicts these high  $Pe$  values for  $\alpha$ .

In the low  $Pe$  limit, the thermal fluctuations dominate. Hence not only the tracer, but also the host particles are effectively passive. The observation of  $\alpha < 1$  at these low Péclet numbers is in agreement with literature. Indeed, for passive colloidal systems subdiffusion of a tracer particle is observed [4]. On the other hand, also the observation  $\alpha > 1$  at high  $Pe$  is consistent with literature. For instance, Wu and Libchaber [8] describe an experiment with passive polystyrene beads in two-dimensional (active) bacterial baths. They find

Table 5.1: Values for the anomalous exponent  $\alpha$  at high Péclet number for different area fractions  $f$ .

$f$	$\alpha_0$
0.079	$1.65 \pm 0.02$
0.393	$1.84 \pm 0.02$
0.628	$1.89 \pm 0.03$

that two diffusion regimes: at short times, the tracer’s motion is superdiffusive, with  $\text{MSD} \sim t^\alpha$  with  $\alpha \in [1.5, 2.0]$ . At long times, the MSD is linear in time. In an attempt to explain this behaviour, a model is proposed by Grégoire et al. [9]. The bacteria are modelled as active Brownian particles. However, their direction is determined by the direction of their neighbours: their angle is the average of the angle of their neighbours plus a stochastic term. This way, ‘swarming’ occurs, in which the bacteria move collectively. This model explains the MSD profile that is observed in [8] well; numerical simulations indicate anomalous diffusion of the tracer with exponent  $\sim 1.65$  at short times and a crossover normal diffusion at long times.

However, in the model we use, the active particles do not (explicitly) align their directions, but we still observe superdiffusion of the tracer at intermediate times. Ref. [24] reports the results of an experiment that is similar to that described in [8], but with algae instead of bacteria. Algae are active as well, but do not swarm as bacteria do, and therefore are a better physical example of the system under investigation in this report than bacteria are. Again, the diffusive behaviour of passive tracer particles is measured. The results are the similar to those measured by in [8]. Moreover,  $\text{MSD}(t)$  increases monotonically with particle concentration. Finally, in [25] the results of simulations of a very similar system are presented, with similar trends as in this report; the anomalous exponent is found to increase with activity and area fraction.

### 5.3 Long-time regime

As  $t \rightarrow \infty$ , the MSD becomes linear in time again. However, the proportionality constant can differ significantly from the diffusion coefficient at short times. Figure 5.3 depicts the ratio of long-time effective diffusion coefficient to short-time diffusion coefficient. We will write  $D_{\text{eff}}$  and  $D_0$  for the long- and short-time diffusion coefficient respectively, and we define

$$\beta := \frac{D_{\text{eff}}}{D_0}. \quad (5.6)$$

Interestingly, now  $\beta$  levels off at *low* Péclet number, to a value that depends on the density. As Pe increases above 1,  $\beta$  increases approximately linearly with Pe. The slopes of this linear relation between  $\beta$  and Pe are displayed in Table 5.2.

At low Pe,  $\beta < 1$ . Hence  $D_{\text{eff}} < D_0$  and the tracer’s diffusivity is lowered by the presence of the crowded environment. This is consistent with literature [4, 26]. Thus, in the long-time limit, the tracer diffuses more slowly than it would if it could diffuse freely. This can qualitatively be explained as follows

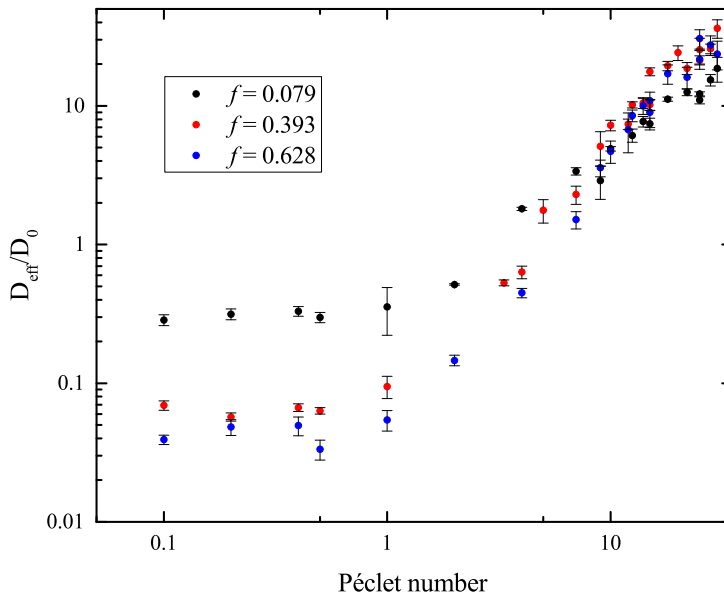


Figure 5.3: Ratio of long-time effective diffusion constant to short-time diffusion coefficient against Péclet number.

[27, 28]: due to the high area fraction, the tracer is ‘caged’ between the host particles, which hinder its self-diffusion. These cages have a finite lifetime  $\tau$ . After this time, the tracer breaks out of the cage and another cage forms around the tracer. When  $t \gg \tau$ , the tracer has moved through many cages. On this coarse time scale, the motion of the tracer and the bath particles is uncorrelated, so that the tracer’s MSD becomes linear again.

A similar argument may explain the dramatic enhancement in diffusivity when  $Pe > 1$  [25]. Now, the tracer is still stuck between hosts; however, the cage formed by the hosts moves with some effective velocity. Hence, the tracer travels a large distance within the cage’s characteristic lifetime. Analogous to the passive case, for  $t \gg \tau$  the motion of the particles becomes uncorrelated, resulting in a linear MSD.

At low area fractions, hydrodynamic interactions are hypothesised to be responsible for the significant enhanced effective diffusion coefficient [8, 29]. Although we must take into account that both these works are concerned with bacteria, that may show swarming behaviour, we can conclude that hydrodynamic interactions are not a necessary condition for enhanced diffusion at high area fractions. This observation is also consistent with other literature [12, 25].

We would like to draw an analogy with a single active particle. Its MSD is given by (2.65):

$$\text{MSD}(t) = \left(4D_T + \frac{2v_0^2}{D_R}\right)t + \frac{2v_0^2}{D_R^2}(\exp(-tD_R) - 1). \quad (5.7)$$

Table 5.2: Slope of  $\beta := D_{\text{eff}}/D_0$  against Pe for  $\text{Pe} \geq 5$ , for different area fractions  $f$ .

$f$	slope
0.079	$0.60 \pm 0.06$
0.393	$1.08 \pm 0.06$
0.628	$1.2 \pm 0.1$

Hence, for  $t \gg 1/D_{\text{R}}$ , the MSD's slope is

$$\frac{d}{dt}\text{MSD}(t) \approx \left(4D_{\text{T}} + \frac{2v_0^2}{D_{\text{R}}}\right) =: 4D_{\text{eff}}^{\text{active}}. \quad (5.8)$$

Moreover, there are constants  $\gamma$  and  $\delta$  such that

$$D_{\text{T}} = \gamma T \quad \text{and} \quad D_{\text{R}} = \delta T. \quad (5.9)$$

If we substitute these expressions in (5.8), and divide by the translational diffusivity  $D_{\text{T}}$ , we find

$$\beta^* := \frac{D_{\text{eff}}^{\text{active}}}{D_{\text{T}}} = 1 + \frac{1}{2} \frac{1}{\gamma\delta} \frac{v_0^2}{T^2} = 1 + \frac{1}{2} \text{Pe}^2, \quad (5.10)$$

where we have used that

$$\text{Pe} = \frac{v_0}{\sqrt{D_{\text{T}}D_{\text{R}}}} = \frac{1}{\sqrt{\gamma\delta}} \frac{v_0}{T}. \quad (5.11)$$

The quantity  $\beta^* = D_{\text{eff}}^{\text{active}}/D_{\text{T}}$  is analogous to  $\beta = D_{\text{eff}}/D_0$ , defined in (5.6). Hence, when  $\text{Pe} \ll 1$ ,  $\beta^*$  is constant. On the other hand, when  $\text{Pe}$  is large,  $\beta^*$  is quadratic in  $\text{Pe}$ .

Analogously, we have seen that  $\beta$  is constant at low  $\text{Pe}$ . At high  $\text{Pe}$ ,  $\beta$  increases with  $\text{Pe}$ , as does  $\beta^*$ , although  $\beta$  seems to increase linearly with  $\text{Pe}$  rather than quadratically. Hence, the tracer inherits many of the properties of the active particles in its environment.

## Chapter 6

# Conclusion and Outlook

We have investigated the dynamics of a passive tracer particle in a crowded, active bath, by examining its MSD. This is done in two ways: analytically and numerically. In both cases, we find that the tracer's diffusion is significantly enhanced by the presence of the active bath. In the following section, we further compare the analytical and numerical results.

### 6.1 Comparison of the analytical and simulation results

The analytical derivations outlined in Chapter 4 predict that the tracer's MSD is linear in time at short times. These dynamics are indeed consistent with the numerical simulations in Chapter 5. However, the analytically predicted long-time ballistic motion is *not* observed in the simulations, which predict normal diffusion at these time scales. The Fokker-Planck equation (4.55) gives rise to an effective stochastic differential equation for the tracer's position  $\mathbf{Z}_t$  such as

$$d\mathbf{Z}_t = \rho\boldsymbol{\Xi} dt + \sqrt{2}\sigma d\mathbf{B}_t, \quad (6.1)$$

i.e. an SDE with constant drift and diffusion terms  $\rho\boldsymbol{\Xi}$  and  $\sqrt{2}\sigma$  respectively. This constant drift term gives rise to the ballistic term in the analytical MSD. The prediction of ballistic motion will be inevitable when using the steady-state approximation, since the ballistic coefficient  $\rho^2|\boldsymbol{\Xi}|^2$  is independent of space and time, and is nonnegative. The drift term being constant is unphysical; it is a result of the omission of time dependence and angular diffusion of the host particles.

Nevertheless, the analytical approximation for the tracer's MSD (4.73) does make some more predictions that are consistent with the observations from simulations. First, the MSD increases with velocity  $v_0$  and decreases with temperature  $T$ . The figures in Chapter 5, in particular Figure 5.3, show similar behaviour; indeed, this is characterised by the Péclet number. Also, the function  $I_1$ , that appears in the expression for  $|\boldsymbol{\Xi}|^2$ , depends only on  $v_0/\sigma^2 = v_0/T$ . Some care is needed when interpreting this dependence, since the Péclet number is given by  $Pe \sim v_0/\sigma\nu$ , and the fact that the quantity  $v_0/T$  coincides with  $Pe$  is only a result of the choice  $\sigma = \nu = \sqrt{T}$  (or equivalently  $D_T = D_R = T$ ) for the

simulations. Also,  $|\Xi|^2$  cannot be written as a function of  $Pe$  only, rather than as a function of both  $v_0$  and  $\sigma^2$ . Hence  $Pe$  is insufficient to completely describe the analytical prediction of the tracer’s enhanced diffusivity. Moreover, the dramatic increase of  $|\Xi|^2$  with  $v_0$  for fixed  $\sigma^2$ , of 5 to even 20 orders of magnitude, as seen in Figure 4.1, is clearly not observed in the numerical experiments.

Moreover, (4.73) predicts an increase of the MSD with density  $\rho$  (or equivalently area fraction  $f$ ). Although the dependence of the MSD on the density is less pronounced than its dependence on the Péclet number, the analytical prediction is partially consistent with the simulation results. At low  $Pe$ , the tracer’s diffusivity is lower than the diffusivity of a freely diffusing particle, but at high  $Pe$  the diffusivity is actually significantly increased. However, (4.73) predicts that the MSD increases with  $\rho$  for any  $Pe$ . This is the result of the omission of host-host interactions in the marginal distribution function (4.51); these interactions create the cages that are responsible for the decrease in the tracer’s diffusivity. Furthermore, the ballistic coefficient  $\rho^2|\Xi|^2$  is unbounded. On physical grounds, one may expect the motion of all particles to decline after some critical density, because the system becomes glassy or crystallises. For example, the analytical approximation predicts ballistic motion (and enhanced diffusion) even at densities such that the area fraction is above 1. We expect that the aforementioned discrepancies between the analytical and numerical approaches are the result of the series of approximations that was necessary to simplify the system of equations.

## 6.2 Outlook

Something that has not been addressed in this report is the dependence of the tracer’s MSD on the size of the tracer. A numerical evaluation of the coefficient  $|\Xi|^2$  shows that it increases with  $\sigma_{AT}$  in an even more dramatic fashion than it does with  $v_0$ . More numerical simulations, for different values of  $\sigma_{AT}$  are necessary to verify whether or not this prediction is accurate, i.e. whether a large tracer indeed diffuses faster than a small one. Moreover, the diffusion coefficients  $D_T$  and  $D_R$  are equal for all types of particles and only depend on temperature, so that  $Pe \sim v_0/T$ . Making  $D_T$  and  $D_R$  depend on other factors, such as the particle size, may shed more light on the relations between  $\alpha$  and  $\beta$  and the Péclet number.

Improving the analytical predictions could start by describing the interactions of the tracer with multiple particles simultaneously. A possible method for this has been outlined in Section 4.4. Further evaluation of the constant  $\Xi'$  found in that Section may provide new information on the tracer’s diffusion. However, incorporating time dependence in the description of the host’s probability density function will be essential in order to elucidate the origins of the values of the anomalous exponent and the long-time effective diffusion coefficient.

The slopes displayed in Table 5.2 are very close, in particular at the two highest area fractions. Further investigation is necessary to know whether these slopes are universal and otherwise how they depend on the area fraction. Furthermore, these slopes are found under the assumption that  $\beta \sim Pe$ . Further investigation is needed in order to make this assumption more rigorous, or to find a more accurate description of the relation between  $\beta$  and  $Pe$ , possibly de-

pending on the area fraction. Moreover, we have seen that  $\alpha_0$ , the high-Pe value of the anomalous exponent  $\alpha$ , increases with area fraction. Further research is necessary to indicate if this increase continues at higher area fractions, or if there is a limiting value for  $\alpha_0$ . One would suppose this limiting value to equal 2, but it could be the case that the system crystallises at an area fraction that is lower than the area fraction at which the tracer would hypothetically show this ballistic motion.

Furthermore, the times between transitions to different diffusive regimes have not been addressed in this work. Since we explain the enhanced tracer diffusion by the concept that the tracer is pushed by a cage of active particles, we speculate that the duration of the superdiffusive regime is related to the lifetime of such a cage. Furthermore, we speculate that the lifetime of a cage is related to the reorientation time of the particles that constitute the cage. Since the reorientation time of an active particle is given by [1, 30]  $1/D_R \sim 1/T$ , we expect that the lifetime of a cage, and therefore also the duration of the superdiffusive regime, decreases with temperature. Moreover, this reasoning implies that the lifetime is independent of the velocity  $v_0$ . Further research is necessary in order to confirm or reject this hypothesis.

# Bibliography

- [1] Clemens Bechinger, Roberto Di Leonardo, Hartmut Löwen, Charles Reichhardt, Giorgio Volpe, and Giovanni Volpe. Active Particles in Complex and Crowded Environments. *Reviews of Modern Physics*, 88(4), nov 2016. doi: 10.1103/revmodphys.88.045006.
- [2] Jędrzej Szymanski and Matthias Weiss. Elucidating the Origin of Anomalous Diffusion in Crowded Fluids. *Physical Review Letters*, 103(3), jul 2009. doi: 10.1103/physrevlett.103.038102.
- [3] Benjamin M. Regner, Dejan Vučinić, Cristina Domnisoru, Thomas M. Bartol, Martin W. Hetzer, Daniel M. Tartakovsky, and Terrence J. Sejnowski. Anomalous Diffusion of Single Particles in Cytoplasm. *Biophysical Journal*, 104(8):1652–1660, apr 2013. doi: 10.1016/j.bpj.2013.01.049.
- [4] Felix Höfling and Thomas Franosch. Anomalous transport in the crowded world of biological cells. doi: 10.1088/0034-4885/76/4/046602.
- [5] Gautam I. Menon. Active Matter. 2010. arXiv: 1003.2032v1.
- [6] Craig W. Reynolds. Flocks, herds and schools: A distributed behavioral model. *SIGGRAPH Comput. Graph.*, 21(4):25–34, August 1987. ISSN 0097-8930. doi: 10.1145/37402.37406.
- [7] Chantal Valeriani, Martin Li, John Novosel, Jochen Arlt, and Davide Marenduzzo. Colloids in a bacterial bath: simulations and experiments. *Soft Matter*, 7:5228–5238, 2011. doi: 10.1039/C1SM05260H.
- [8] Xiao-Lun Wu and Albert Libchaber. Particle Diffusion in a Quasi-Two-Dimensional Bacterial Bath. *Physical Review Letters*, 84:3017–3020, Mar 2000. doi: 10.1103/PhysRevLett.84.3017.
- [9] Guillaume Grégoire, Hugues Chaté, and Yuhai Tu. Active and passive particles: Modeling beads in a bacterial bath. *Physical Review E*, 64(1), jun 2001. doi: 10.1103/physreve.64.011902.
- [10] Yi Peng, Lipeng Lai, Yi-Shu Tai, Kechun Zhang, Xinliang Xu, and Xiang Cheng. Diffusion of Ellipsoids in Bacterial Suspensions. *Physical Review Letters*, 116:068303, Feb 2016. doi: 10.1103/PhysRevLett.116.068303.
- [11] Gastón Miño, Thomas E. Mallouk, Thierry Darnige, Mauricio Hoyos, Jeremi Dauchet, Jocelyn Dunstan, Rodrigo Soto, Yang Wang, Annie Rousselet, and Eric Clement. Enhanced Diffusion due to Active Swimmers at a Solid Surface. *Physical Review Letters*, 106:048102, Jan 2011. doi: 10.1103/PhysRevLett.106.048102.
- [12] Eric W. Burkholder and John F. Brady. Tracer diffusion in active suspensions. *Phys. Rev. E*, 95:052605, May 2017. doi: 10.1103/PhysRevE.95.052605.
- [13] Kiyoshi Kanazawa, Tomohiko G. Sano, Andrea Cairoli, and Adrian Baule.



- Loopy Lévy flights enhance tracer diffusion in active suspensions. *Nature*, 579(7799):364–367, mar 2020. doi: 10.1038/s41586-020-2086-2.
- [14] Jan Dhont. *An Introduction to Dynamics of Colloids*. Elsevier, 1996. ISBN 9780444820099.
- [15] Bernt Øksendal. *Stochastic Differential Equations*. Springer, sixth edition, 2003. ISBN 978-3540047582.
- [16] Grigorios Pavliotis. *Stochastic Processes and Applications: Diffusion Processes, the Fokker-Planck and Langevin Equations*. Springer, New York, NY, 2014. ISBN 9781493913237.
- [17] Masao Doi and Sam F. Edwards. *The Theory of Polymer Dynamics*. Clarendon Press, 1986. ISBN 9780198520337.
- [18] Andrey N. Kolmogorov and Sergei V. Fomin. *Elements of the Theory of Functions and Functional Analysis [Two Volumes in One]*. Martino Fine Books, 2012. ISBN 1614273049.
- [19] Walter Kob and Hans C. Andersen. Scaling Behavior in the  $\beta$ -Relaxation Regime of a Supercooled Lennard-Jones Mixture. *Physical Review Letters*, 73:1376–1379, Sep 1994. doi: 10.1103/PhysRevLett.73.1376.
- [20] Ralf Brüning, Denis A St-Onge, Steve Patterson, and Walter Kob. Glass transitions in one-, two-, three-, and four-dimensional binary lennard-jones systems. *Journal of Physics: Condensed Matter*, 21(3):035117, dec 2008. doi: 10.1088/0953-8984/21/3/035117.
- [21] Eckhard Platen Peter E. Kloeden. *Numerical Solution of Stochastic Differential Equations*. Springer-Verlag Berlin Heidelberg, 1992. ISBN 978-3-540-54062-5.
- [22] J. T. Chang and D. Pollard. Conditioning as disintegration. *Statistica Neerlandica*, 51(3):287–317, nov 1997. doi: 10.1111/1467-9574.00056.
- [23] Milton Abramowitz and Irene A. Stegun. *Handbook of Mathematical Functions*. Dover Publications Inc., ninth edition, 1965. ISBN 0486612724.
- [24] Hüseyin Kurtuldu, Jeffrey S. Guasto, Karl A. Johnson, and J. P. Gollub. Enhancement of biomixing by swimming algal cells in two-dimensional films. *Proceedings of the National Academy of Sciences*, 108(26):10391–10395, 2011. ISSN 0027-8424. doi: 10.1073/pnas.1107046108.
- [25] Chen Wang and Hongyuan Jiang. The inhibition of concentrated active baths. *The Journal of Chemical Physics*, 152(18):184907, 2020. doi: 10.1063/5.0005313.
- [26] Firoozeh Babayekhorasani, Dave E. Dunstan, Ramanan Krishnamoorti, and Jacinta C. Conrad. Nanoparticle diffusion in crowded and confined media. *Soft Matter*, 12(40):8407–8416, 2016. doi: 10.1039/c6sm01543c.
- [27] Eric R. Weeks and David A. Weitz. Subdiffusion and the cage effect studied near the colloidal glass transition. *Chemical Physics*, 284(1):361–367, 2002. ISSN 0301-0104. doi: 10.1016/S0301-0104(02)00667-5. Strange Kinetics.
- [28] Henk N. W. Lekkerkerker and Jan K. G. Dhont. On the calculation of the self-diffusion coefficient of interacting Brownian particles. *The Journal of Chemical Physics*, 80(11):5790–5792, 1984. doi: 10.1063/1.446602.
- [29] Andrey Sokolov, Igor S. Aranson, John O. Kessler, and Raymond E. Goldstein. Concentration Dependence of the Collective Dynamics of Swimming Bacteria. *Physical Review Letters*, 98:158102, Apr 2007. doi: 10.1103/PhysRevLett.98.158102.
- [30] Wen Yan and John F. Brady. The force on a boundary in active matter. *Journal of Fluid Mechanics*, 785:R1, 2015. doi: 10.1017/jfm.2015.621.